

PVP2008-61602

ROBUST ENGINEERING DESIGN FOR FAILURE PREVENTION (*)

Jeffrey T. Fong

Mathematical & Computational Sciences Division
National Institute of Standards & Tech. (NIST)
Gaithersburg, MD 20899-8910 USA
fong@nist.gov

James J. Filliben

Statistical Engineering Division
National Institute of Standards & Tech. (NIST)
Gaithersburg, MD 20899-8980 USA
filliben@nist.gov

N. Alan Heckert

Statistical Engineering Division
National Institute of Standards & Tech. (NIST)
Gaithersburg, MD 20899-8980 USA
alan.heckert@nist.gov

Roland deWit

Metallurgy Division
National Institute of Standards & Technology (NIST)
Gaithersburg, MD 20899 USA
deWit@nist.gov

Barry Bernstein

Dept. of Chemical & Environmental Engineering
and Department of Mathematics
Illinois Institute of Technology
Chicago, IL 60616
bernsteinb@iit.edu

ABSTRACT

To advance the state of the art of engineering design, we introduce a new concept on the "robustness" of a structure by measuring its ability to sustain a sudden loss of a part without causing an immediate collapse. The concept is based on the premise that most structures have built-in redundancy such that when the loss of a single part leads to a load redistribution, the "crippled" structure tends to seek a new stability configuration without immediate collapse. This property of a "robust" structure, when coupled with a continuous or periodic inspection program using nondestructive evaluation (NDE) techniques, is useful in failure prevention, because such structure is expected to display "measurable" signs of "weakening" long before the onset of catastrophic failure. To quantify this "robustness" concept, we use a large number of simulations to develop a metric to be named the "Robustness Index (RBI)." To illustrate its application, we present two examples: (1) the design of a simple square grillage in support of a water tank, and (2) a classroom model of a 3-span double-

Pratt-truss bridge. The first example is a "toy" problem, which turned out to be a good vehicle to test the feasibility of the RBI concept. The second example is taken from a textbook in bridge design (Tall, L., *Structural Steel Bridge*, 2nd ed., page 99, Fig. 4.3(b), Ronald Press, New York NY, 1974). It is not a case study for failure analysis, but a useful classroom exercise in an engineering design course. Significance and limitations of this new approach to catastrophic failure avoidance through "robust" design, are discussed.

Keywords: Aging structures; analysis of variance; applied mechanics; bridge design; design of experiments; engineering safety; error propagation; finite element method; NDE monitoring; RBI; robust design; robustness index; robustness metric; sensitivity analysis; statistical data analysis; structural robustness analysis; uncertainty analysis.

Disclaimer: The views expressed in this paper are strictly those of the authors and do not necessarily reflect those of their affiliated institutions. The mention of names of all commercial vendors and their products is intended to illustrate the capabilities of existing products, and should not be construed as endorsement by the authors or their affiliated institutions.

(*) Contribution of the U.S. National Institute of Standards and Technology (NIST). Not subject to copyright.

1. INTRODUCTION

Engineers and engineering educators have been interested in better methods of design and more reliable procedures of operation and maintenance of structures and components for a long time. In particular, to prevent catastrophic failures of high-consequence structural systems, new approaches to evaluating the "vulnerability" of such systems, and enhancing their "inspectability" by continuous monitoring using nondestructive evaluation (NDE) methods would be of great interest.

Before the arrival of computers, engineers designed by mathematical modeling and analysis, and evaluate their designs using functional, economic, and safety criteria with the help of engineering judgment and codes and standards. Since the 1950s, computers and numerical modeling have become powerful tools in engineering design, and codes and standards have changed enormously to accommodate societal needs for newer functionality, more efficient economics, and better safety, but the method of design evaluation has remained the same, namely, it did not include an examination of the "vulnerability" of the design using computer modeling and simulation of potential failure scenarios.

To illustrate the evolution in engineers' thinking on this subject, we first quote two comments from the literature of the 1980s and 1990s. In 1983, at the International Conference on Structure Failure, Product Liability and Technical Insurance, Rossmanith [1] stated:

"... engineers need to be familiar with all possible failure inducing parameters before committing to a product design and manufacturing (construction) plan."

In 1991, Piesold remarked in the preface of his book [2]:

"... engineering works seldom collapse or fail to perform because there has been an error in calculations—such occurrences are uncommon—but more frequently because of the advent or existence of some seemingly minor circumstances which does not appear to merit special consideration during the implementation of the project."

We underline two words in those comments to emphasize their diametrically opposite views, i.e., Rossmanith [1] urged engineers to invoke failure analysis before design, and Piesold [2] wrote from experience that such failure analysis, if ever performed before design, would not do much good anyway.

Advances in engineering research in the 1980s provided two new tools to resolve this dilemma. The first was fracture mechanics. As Kanninen remarked in the preface of his 1985 book [3]:

"... Enough research (in fracture mechanics) has been

performed to provide a solid foundation upon which future progress will build. At the same time, societal dictates for optimum uses of energy and materials are increasingly forcing structural integrity assessments to be made in the more realistic way afforded by a fracture mechanics approach." (Underlines added by this author.)

The second was the use of nondestructive evaluation (NDE) methods for flaw detection, location, and sizing. In March 21-25, 1983, Bush [4] addressed a technical session of the International Symposium on Reliability of Reactor Pressure Components, IAEA, Stuttgart, Germany, with the following:

"... Reliability of flaw detection, sizing, and location represents a critical input in the overall assessment of nuclear systems and components comprising the pressure boundary. For example, a relatively benign flaw detected early in plant life can be evaluated by approved fracture mechanics techniques and permitted to remain indefinitely, subject to periodic monitoring, thus resulting in little or no perturbation in plant operation, plus generation of confidence in the safety authorities that the plant organization used "good" nondestructive examination procedures." (Underlines added for emphasis by this author.)

Both tools, however, came into play only after a design was finalized, a structure or component was manufactured, and a system was placed into service. Neither tool addressed a significant question related to failure prevention, i.e.,

"Is a design 'robust' enough for a structure or component to sustain a loss of a part without catastrophic failure?"

The purpose of this paper is to address this "robustness" question by introducing a new approach to design evaluation. We emphasize that this new approach is *in addition to* and *not in lieu of* the traditional method of assessing a design. In Section 2, we define the concept of a "Robustness Index (RBI)" and develop a procedure to calculate it with an example on the design of a square grillage in support of a water tank². In Section 3, we present a finite element analysis of a classroom model of a 3-span double-Pratt-truss bridge based on Tall [5, p. 99]. In the first example of Section 2, we used a public-domain statistical data analysis package named DATAPLOT [6]. For the second example of Section 3, we used a student edition (se) of a finite element analysis code named ABAQUS [7] and several alternative designs of the 466-element, 141-node model structure to motivate an application of the robustness metric. A discussion of the significance and limitations of this new approach, a conclusion, an acknowledgment, and references appear in Sections 4 through 7, respectively. Two sample computer input files, one using DATAPLOT, and the other, ABAQUS-se, are included as Appendix A and B, respectively.

²The use of a "toy" problem was critical in developing the idea of RBI.

¹Number in brackets denotes a reference listed at the end of this paper.

2. "ROBUSTNESS INDEX (RBI)"

To answer the question posed in the last section, we introduce a concept on the "robustness" of a structure by measuring its ability to sustain a sudden loss of a part without causing a total collapse, i.e., a catastrophic failure.

The concept is based on the premise that most structures have built-in redundancies such that when the loss of a single part leads to a local load redistribution, the "crippled" structure tends to seek a new stability configuration without immediate collapse. This nice property of a "robust" structure, when coupled with a continuous or periodic inspection program

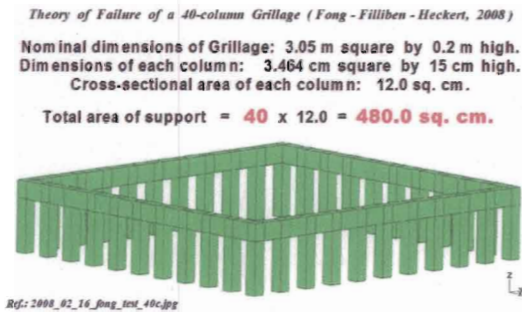


Fig. 1. A perspective view of a 40-column square grillage designed to support the weight of a water tank on top as the tank is being filled up at the rate of 1 unit load per minute.

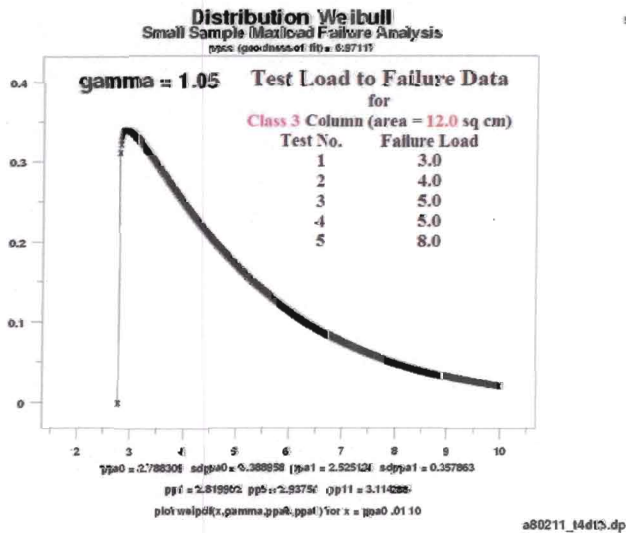


Fig. 2. A Weibull distribution fit of the data from five compressive strength tests for a specific class of columns designed for the 40-column grillage such that the cross-sectional area of each column is 12.0 sq cm and the mean failure strength per column is 5.0 load units.

using nondestructive evaluation (NDE) techniques, is extremely desirable in preventing high-consequence failures, because such structures are expected to display "measurable" signs of "weakening" long before the onset of catastrophic failure.

Let N be the number of simulations we choose to perform on a specific failure scenario of a given structure. For simplicity, let us begin by assuming that the structure can be broken down into M identical elements of equal strength. Each simulation is conducted as a "virtual experiment" on the progressive weakening of that M -member structure, i.e., when one of the members of the structure fails, the load is redistributed to its remaining $M-1$ members, and when a second member fails, the load is redistributed again to its $M-2$ members, and so on, until the structure collapses at some number i , $1 \leq i \leq M$.

Let n_1 be the total number of simulations where the structure collapses at the loss of its first member. Let n_2 be the total number of simulations where the structure did not collapse at the loss of its first member, but did collapse at the loss of its second member. For each set of N simulations, we can always find a set of numbers, $n_1, n_2, n_3, \dots, n_x$, such that their sum equals N , and the subscript x is the largest number of the members a structure can lose up to the moment of collapse. Let m be the mean of that set, $(n_1, n_2, n_3, \dots, n_x)$.

This formulation yields two measures relevant to the notion of "robustness." The first measure is the ratio, $(N - n_1) / N$, which can be interpreted as the initial resilience of the structure, or the probability of sustaining the loss of one member without collapse. The second is the ratio, $(M - m) / M$, which can be interpreted as the overall resilience of the structure, or the average percentage of the structure that remains after progressive weakening becomes excessive causing collapse.

We now propose to define the "robustness" of a structure, to be known as the "robustness index (RBI)," as the product of those two ratios and 100, i.e.,

$$RBI = (N - n_1) * (M - m) * 100 / (N * M) \quad (1)$$

In general, RBI varies between 0 and 100, with 0 being the least robust, and 100, the most.

To test the feasibility of this index, we choose to work with a simple problem, i.e., the design of a square grillage with M number of columns in support of a water tank. To fix the geometry of a typical design, let us consider the nominal dimensions of a grillage to be 3.05 m square by 0.2 m in height. In Fig. 1, we display a 40-column grillage with each column being 3.464 cm square by 15 cm in height such that the total area of support is $40 \times 3.464 \times 3.464 = 480$ sq cm. In subsequent designs, we shall hold the total area of support constant and vary the number of columns to see which design has the best "robustness index."

2. "ROBUSTNESS INDEX (RBI)" (Continued)

Stochastic Failure of a 40-column Grillage (Fong-Filliben-Heckert, 2008)

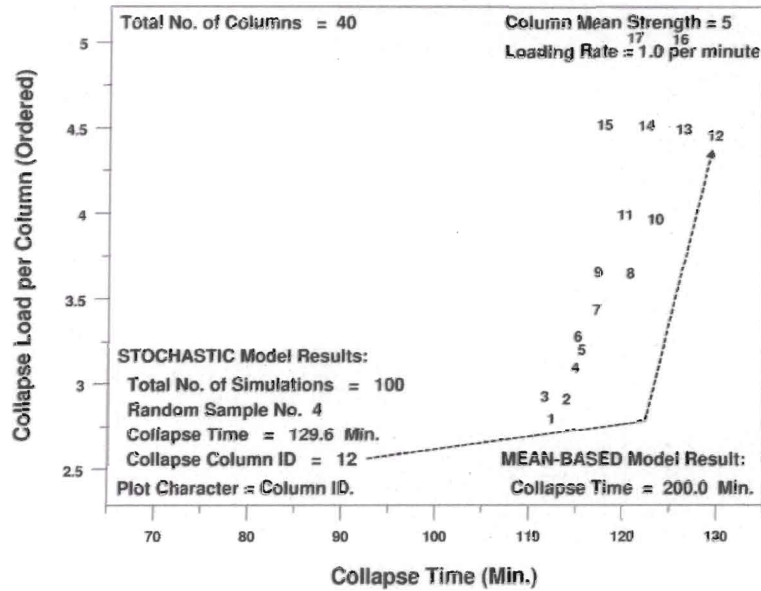


Fig. 3. Simulation No 4 of a stochastic model experiment (N = 100) on the progressive weakening of a 40-column grillage as the water tank on top is being filled at the rate of 1.0 load unit per minute. Note that when the first column, ID-1, failed at about 112 minutes, a load redistribution occurred until about 114 minutes when the second column, ID-2, failed. This is then followed by a simultaneous failure of two columns, ID-3 and ID-4, at about 115 minutes, and so on, until the failure of ID-12 caused the grillage to collapse at 129.6 min. Since the loading rate is 1.0 unit per minute, the failure load is 129.6 load units.

Stochastic Failure of a 40-column Grillage (Fong-Filliben-Heckert, 2008)

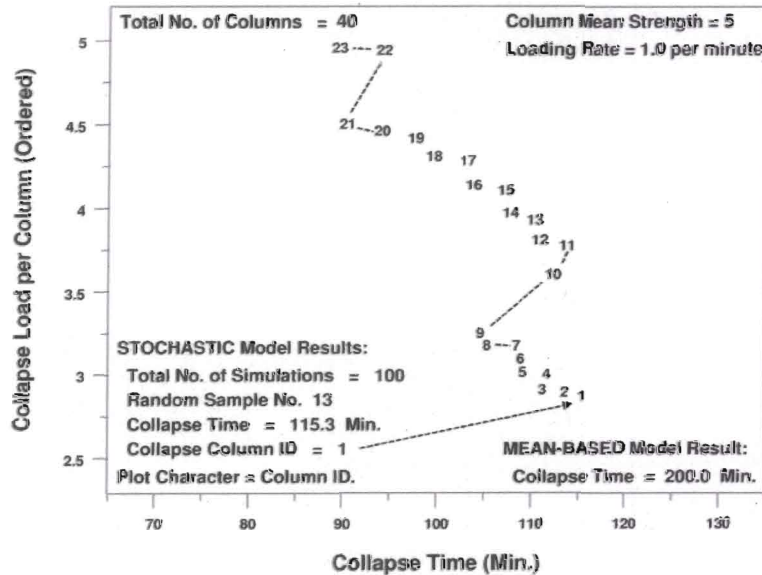


Fig. 4. Simulation No 13 of a stochastic model experiment (N = 100) on the progressive weakening of a 40-column grillage as the water tank on top is being filled at the rate of 1.0 load unit per minute. Note that this simulation happened to result in the grillage collapse at the loss of its first column. The plot clearly shows that subsequent load redistributions after ID-1 failed at 115.3 min. were unable to produce a sequence of loads greater than 115.3 load units.

2. "ROBUSTNESS INDEX (RBI)" (Continued)

Stochastic Failure of a 40-column Grillage (Fong-Filliben-Heckert, 2008)

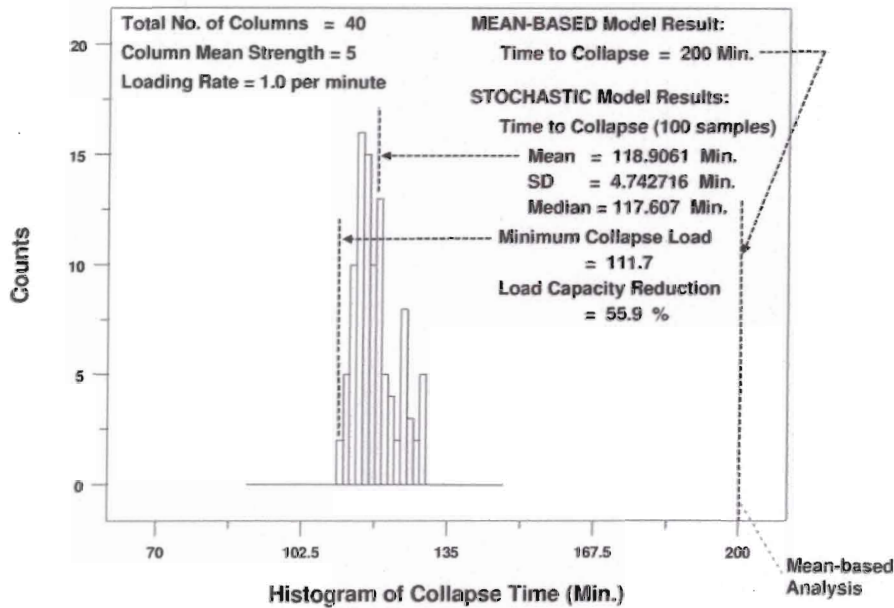


Fig. 5. A histogram of the collapse time of a 40-column grillage in a 100-simulation experiment as the water tank on top is being filled at the rate of 1.0 load unit per minute. Note that a deterministic model with a mean failure strength of 5.0 load units per column predicts a collapse time of $40 \times 5.0 = 200$ min., whereas a stochastic model with a Weibull distribution of the failure strength predicts a minimum and mean collapse loads at 111.7 and 118.9 units, respectively.

Stochastic Failure of a 40-column Grillage (Fong-Filliben-Heckert, 2008)

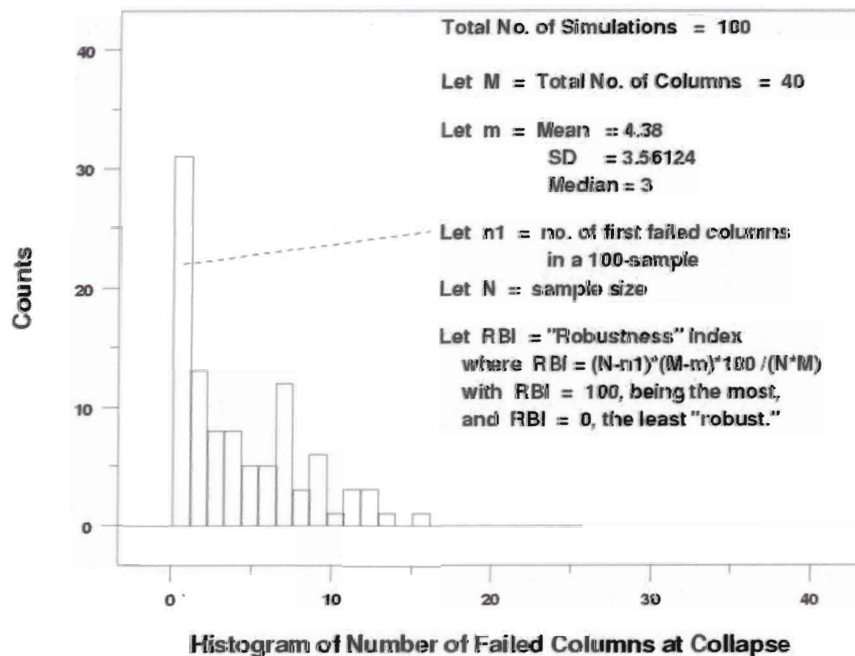


Fig. 6. A histogram of the number of failed columns at collapse for a 100-simulation experiment as the water tank on top is being filled at the rate of 1.0 load unit per minute. Since $N = 100$, $n_1 = 31$, $M = 40$, and $m = 4.38$, the RBI equals 61.4.

2. "ROBUSTNESS INDEX (RBI)" (Continued)

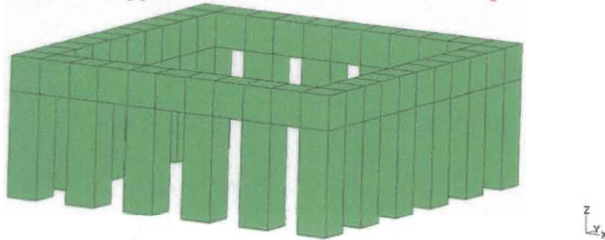
To obtain an estimate of the compressive failure strength of the 40 columns under investigation, we asked a material testing laboratory to make a total of five tests. The results were given in Fig. 2. Again for simplicity, we chose to work with an arbitrary unit of load, and the five test data, 3.0, 4.0, 5.0, 5.0, 8.0, yielded a mean of 5.0 and a standard deviation of 1.87.

Since we work with failure loads which are positive definite, we find the 3-parameter Weibull distribution (see, e.g., Hastings and Peacock [8], Evans, et al [9]) a more suitable representation than the two-parameter Gaussian. Using a public domain statistical data analysis software package named DATAPLOT [7], we varied a few choices of the Weibull shape parameters and used a goodness-of-fit criterion due to Filliben [10] to choose $\gamma = 1.05$, location parameter = 2.7883, and scale parameter = 2.5251 to fit the five test data as shown in Fig. 2.

Theory of Failure of a 20-column Grillage (Fong - Filliben - Heckert, 2008)

Nominal dimensions of Grillage: 3.05 m square by 0.2 m high.
 Dimensions of each column: 4.899 cm square by 15 cm high.
 Cross-sectional area of each column: 24.0 sq. cm.

Total area of support = 20 x 24.0 = 480.0 sq. cm.



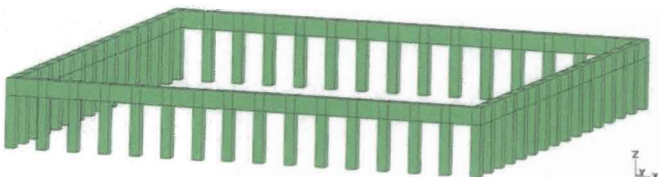
Ref.: 2008_02_16_fong_test_20c.jpg

Fig. 7. A perspective view of a 20-column square grillage designed to support the weight of a water tank on top as the tank is being filled up at the rate of 1 unit load per minute.

Theory of Failure of a 60-column Grillage (Fong - Filliben - Heckert, 2008)

Nominal dimensions of Grillage: 3.05 m square by 0.2 m high.
 Dimensions of each column: 2.828 cm square by 15 cm high.
 Cross-sectional area of each column: 8.0 sq. cm.

Total area of support = 60 x 8.0 = 480.0 sq. cm.



Ref.: 2008_02_16_fong_test_60c.jpg

Fig. 8. A perspective view of a 60-column square grillage designed to support the weight of a water tank on top as the tank is being filled up at the rate of 1 unit load per minute.

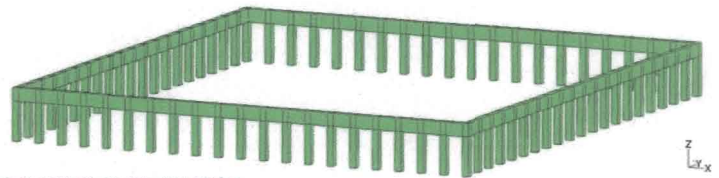
We then wrote an algorithm in DATAPLOT (see Appendix A for a listing of that code) to simulate the progressing weakening of the 40-column grillage using a stochastic model as the water tank on top begins to fill at the rate of 1.0 load unit per minute. For each simulation of this model, we used a random number generator to find 40 failure loads from the Weibull distribution, and plotted the resulting collapsed load per column as an ordered set versus the collapse time as shown in Figs. 3 and 4 for two typical simulations, Nos. 4 and 13, respectively. For a sample size of 100 ($= N$), we plot a histogram of the collapse time in Fig. 5, and the number of failed columns at collapse in Fig. 6. With $n_1 = 31$, $M = 40$, and $m = 4.38$, we found that RBI equals 61.4.

It is interesting to note that the concept of RBI becomes a degenerate case ($= 0$) when applied to this simple problem in a mean-based (deterministic) analysis. That is, when all columns

Theory of Failure of a 80-column Grillage (Fong - Filliben - Heckert, 2008)

Nominal dimensions of Grillage: 3.05 m square by 0.2 m high.
 Dimensions of each column: 2.449 cm square by 15 cm high.
 Cross-sectional area of each column: 6.0 sq. cm.

Total area of support = 80 x 6.0 = 480.0 sq. cm.



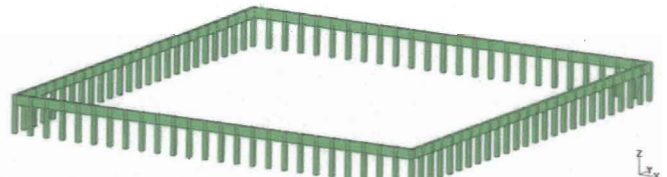
Ref.: 2008_02_16_fong_test_80c.jpg

Fig. 9. A perspective view of a 80-column square grillage designed to support the weight of a water tank on top as the tank is being filled up at the rate of 1 unit load per minute.

Theory of Failure of a 100-column Grillage (Fong - Filliben - Heckert, 2008)

Nominal dimensions of Grillage: 3.05 m square by 0.2 m high.
 Dimensions of each column: 2.191 cm square by 15 cm high.
 Cross-sectional area of each column: 4.8 sq. cm.

Total area of support = 100 x 4.8 = 480.0 sq. cm.



Ref.: 2008_02_16_fong_test_100c.jpg

Fig. 10. A perspective view of a 100-column square grillage designed to support the weight of a water tank on top as the tank is being filled up at the rate of 1 unit load per minute.

2. "ROBUSTNESS INDEX (RBI)" (Continued)

fail simultaneously in a mean-based model, m is indeterminate, and $n_1 = N$, thus making the robustness index, RBI , zero.

We next investigated whether the value of RBI was sensitive to the sample size, N . For a 40-column grillage, we found the following results as N varied from 100 to 2000:

N	n_1	M	m	RBI
100	31	40	4.38	61.4
200	53	40	4.61	64.9
400	125	40	4.413	61.2
1,000	350	40	4.358	57.9
2,000	700	40	4.34	57.9

proportional change of the five test data from (3, 4, 5, 5, 8) to (6, 8, 10, 10, 16), since each of those five data referred to a failure load per column and not per unit support area. The results as listed below and plotted on Fig. 11 indicate that RBI could potentially be a viable metric for "robustness."

N	n_1	M	m	RBI
1,000	395	20	2.889	51.8
1,000	350	40	4.358	57.9
1,000	255	60	5.404	67.8
1,000	250	64	5.70	68.3
1,000	250	68	5.879	68.5
1,000	250	72	6.104	68.6
1,000	225	76	6.386	71.0
1,000	225	80	6.704	71.0
1,000	220	84	6.885	71.6
1,000	220	88	7.168	71.6
1,000	225	92	7.27	72.1
1,000	210	96	7.466	72.9
1,000	225	100	7.672	71.6

For the rest of this investigation, we adopted N to be 1,000, and varied M from 20 to 100 while keeping the total area of support (= 480 sq cm) and the total mean load capacity (= 200 load units) constant. In Figs. 7 through 10, we present four such grillage designs as $M = 20, 60, 80,$ and $100,$ respectively. For example, when $M = 20,$ the cross-sectional area of each column was 24.0 sq cm, and the mean failure load was 10.0 instead of 5.0 for $M = 40.$ This also required a

Theory of "Robust" Engineering Design (Forng-Filliben-Heckert, 2008)

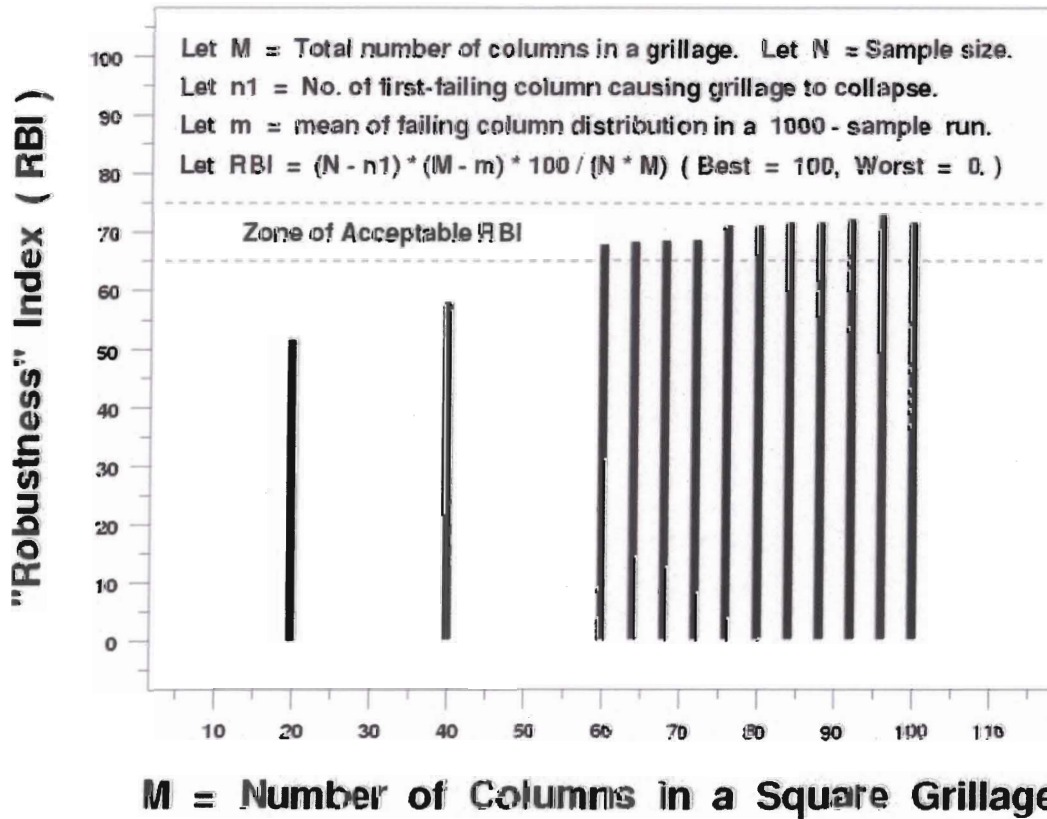


Fig. 11. A plot of the "Robustness Index (RBI)" vs. M , the number of columns in a square grillage, as M varies from 20 to 100, and the sample size, N , equals 1000. Note that after M reaches 60, the growth of RBI begins to slow down. A good choice of M for this investigation is 60.

3. A 466-CHORD DOUBLE-TRUSS BRIDGE

Motivated by a page from a textbook in bridge design by Tall [5, p. 99, Fig. 4.3(b)], we develop in this section a classroom exercise on how to evaluate the "robustness" of a real structure such as a 3-span double-Pratt-truss bridge.

To conduct a "virtual experiment" in a classroom on the collapse of a complex structure such as a truss bridge within the 1000-node limitation of the student edition of a finite element method (FEM) code named ABAQUS [7], we had to introduce a scaled-down geometric model of a real bridge as shown in Fig. 12. It turns out that only 141 nodes and 466 elements are sufficient to describe the geometry of the classroom model as shown in a sample input file given in Appendix B.

To simplify the task of modeling the classroom bridge at, say, 1/12-scale of a real bridge, it is advantageous for us to adopt the U.S. engineering units, i.e., inch., lbf, and psi for length, force,

and stress, respectively, such that a real bridge main span length of, say, 456 ft., can easily be converted to a model main span length of 456 in. For a 12-bay main span, the length of each model upper and lower chord is $456/12 = 38$ in. Let us adopt the geometry of a 3-span classroom bridge as follows:

The Left Approach span has 8 bays at 38 in. each:

$$\text{Total length} = 8 \times 38.0 = 304.0 \text{ in.}$$

The Main span has 12 bays at 38 in. each:

$$\text{Total length} = 12 \times 38.0 = 456.0 \text{ in.}$$

The Right Approach span has 7 bays at 38 in. each:

$$\text{Total length} = 7 \times 38.0 = 266.0 \text{ in.}$$

Continuing the formulation of the geometric model, which we named **Model-1**, we estimate the lengths of all vertical chords of the 3-span bridge by adopting a parabolic function to inter-

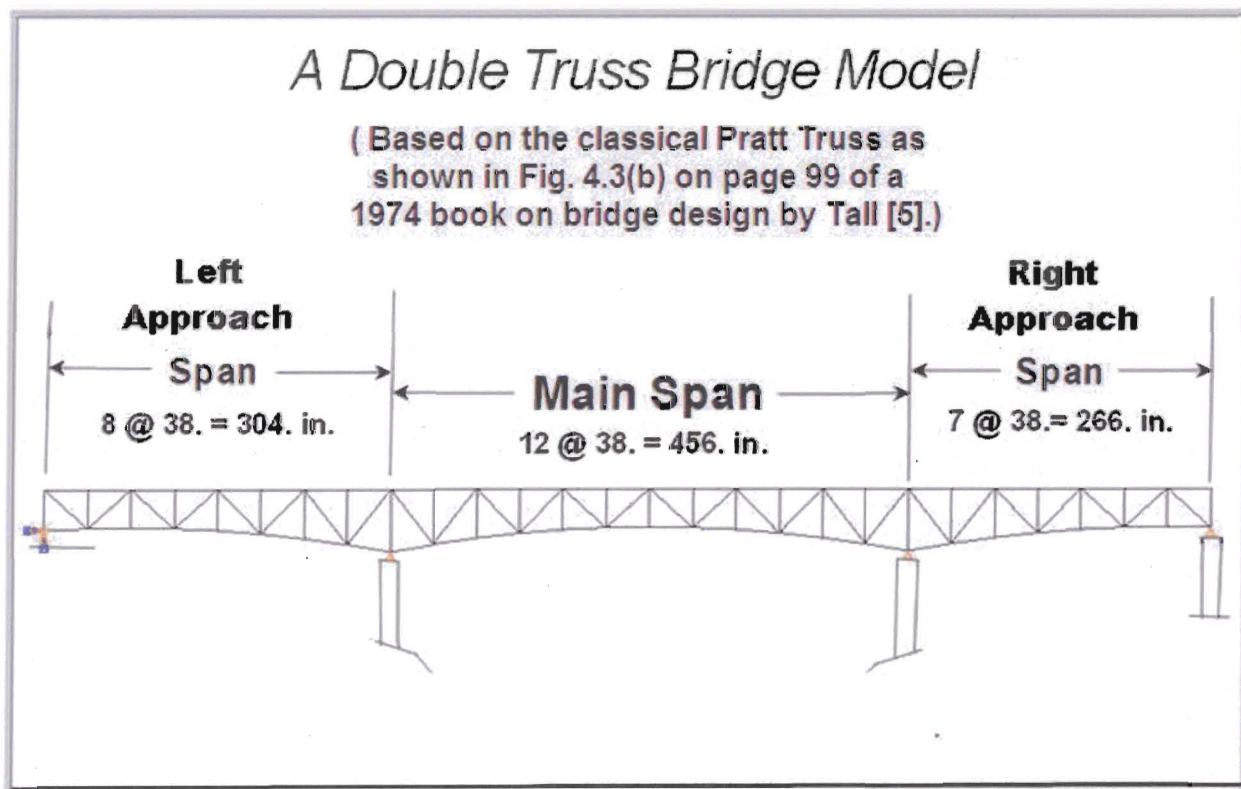


Fig. 12. Elevation of a double-truss bridge, modeled at 1/12-scale of a real 3-span double-Pratt-truss bridge as described in Tall [5, p.99, Fig. 4.3(b)]. Using a student edition of the finite element code ABAQUS, version 6.6-2, we create an input file for this model, namely, **Model-1**, as listed in **Appendix B**.

3. A 466-CHORD DOUBLE-TRUSS BRIDGE (Continued)

polate from a real bridge minimum of 32 ft. to a maximum of 52 ft. This means a model minimum of 32 in. to a maximum of 52 in. For a double-truss bridge, we also assume that the two trusses are connected by laterals with a real bridge spacing of 60 ft., or a model spacing of 60 in. between the two single trusses. We introduce cross braces at each portal between the trusses and in-between each set of portals to add stability. We also add an extra node in the lower chord of each portal as shown in Fig. 13.

Again for simplicity, we assume all chords in **Model-1** are made of draw-quality mild steel with a 1.50 in. square cross section, and two elastic constants given by Young's modulus, E , of 30,000,000 psi and Poisson's ratio, ν , of 0.30. For failure

analysis, we also assume a mean tensile and compressive yield strength, Y , of 36,000 psi (= 36.0 ksi). A third failure criterion is buckling, and we use the Euler formula (see, e.g., Mott [11, pp. 549-562]) to calculate the critical buckling load, P_{Cr} , as follows:

$$P_{Cr} = \pi^2 E A / (L_e / r)^2, \quad (2)$$

where A is the cross-sectional area, L_e , the effective length, and r , the radius of gyration. For a typical pin-connected lower or upper chord of **Model-1**, the effective length of each chord equals its length ($L_e = 38.0$ in.), and with $A = 2.25$ sq in, $r^2 = A/12 = 0.1875$, we obtain $P_{Cr} = 86,500$ lbf from eq. (2).

Finally, we assume the conventional type of boundary condition

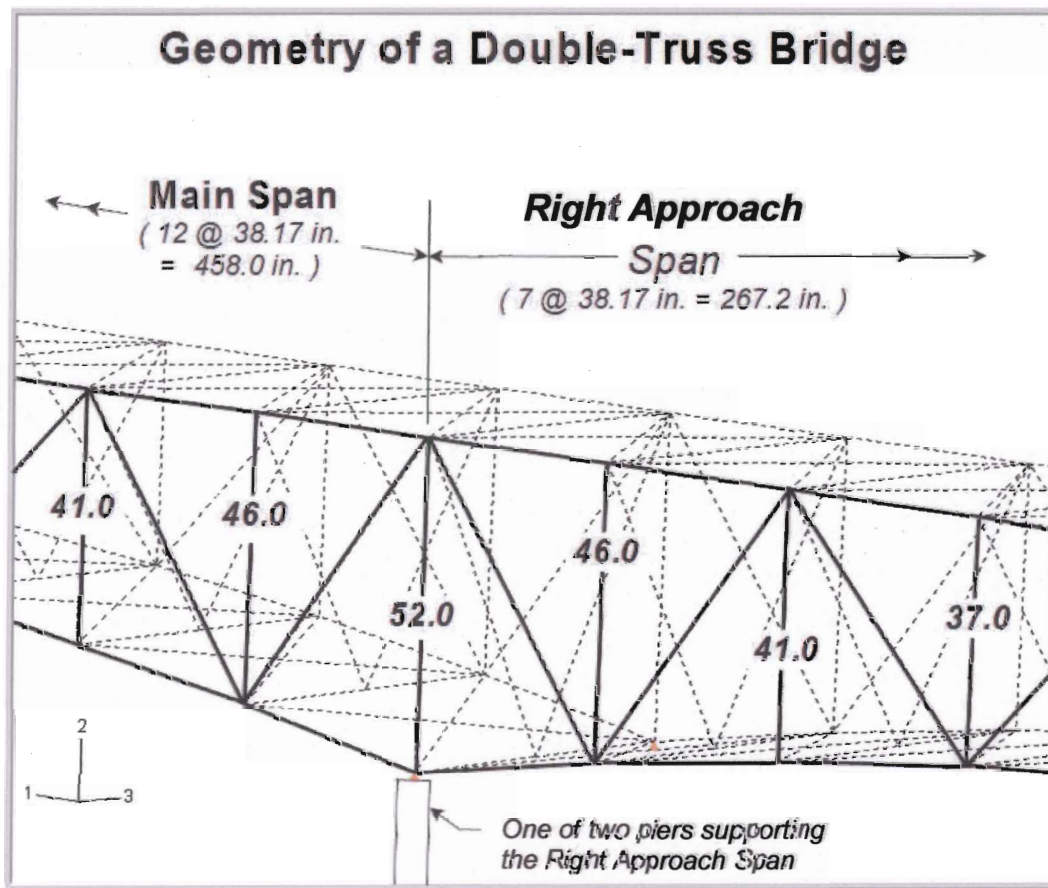


Fig. 13. A perspective view of a portion of the model bridge, **Model-1**, between its Main and Right Approach spans, with lengths of the vertical chords shown in inches. We estimate the vertical chords of the original arch-like truss bridge to have a maximum depth of 52.0 ft. at the support and 32.0 ft. at mid-span. Using a parabolic function, $y = 32 + x^2 / 1.8$, where $x = 0, 1, \dots, 6$, to describe one-half of the arch shape of the Main span, we estimate, to the nearest 0.5 ft., the lengths of the 7 vertical chords from mid-span to support to vary from 32.0, 32.5, 34.0, 37.0, 41.0, 46.0, to 52.0. For the 8-bay Left Approach span, the verticals are 34.0, 32.5, and the seven lengths of the Main span. For the 7-bay Right Approach span, the verticals are 32.5 and the seven lengths of the Main span.

3. A 466-CHORD DOUBLE-TRUSS BRIDGE (Continued)

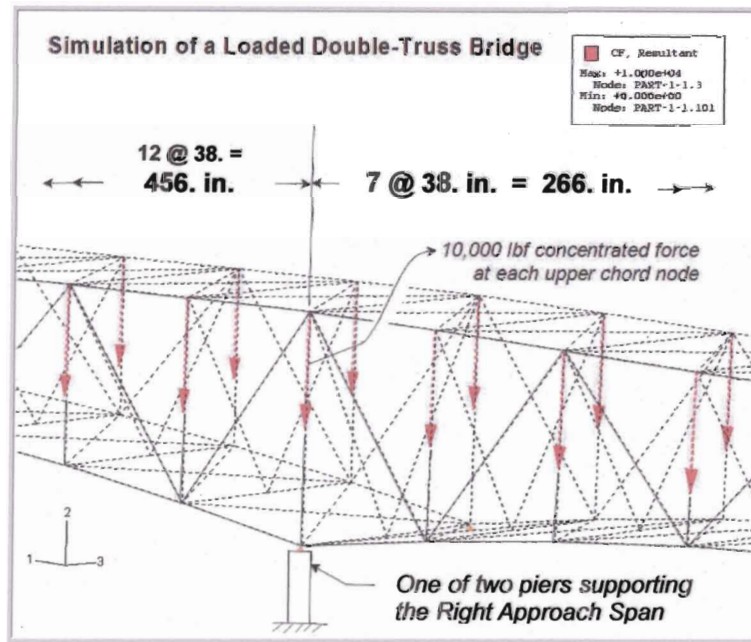


Fig. 14. A perspective view of a portion of the model bridge, **Model-1**, between its Main and Right Approach spans, with a concentrated load of 10,000 lbf applied at each of its upper chord nodes except four at the two ends (not shown), at which only 5,000 lbf is applied.

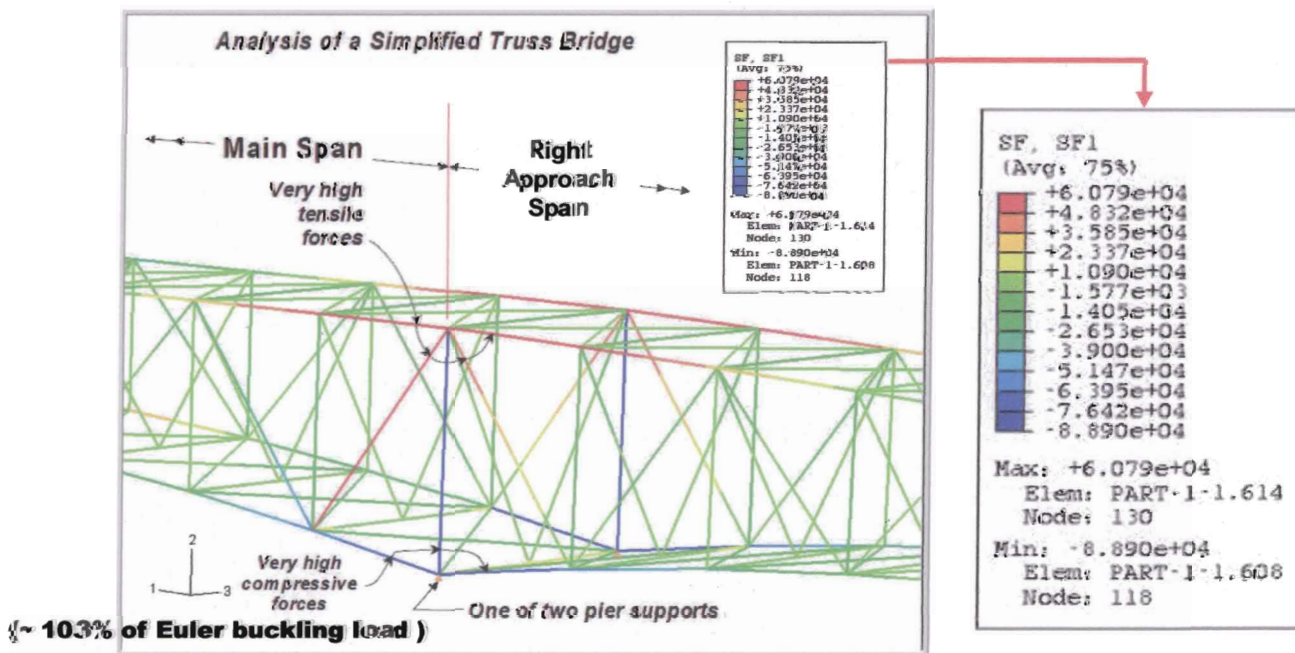


Fig. 15. A perspective view of a portion of the model bridge, **Model-1**, between its Main and Right Approach spans, with results of an analysis by finite element method (ABAQUS, 6.6-2) given in colors, red, orange, yellow being tensile forces, and green, blue, compressive.

3. A 466-CHORD DOUBLE-TRUSS BRIDGE (Continued)

to hold for the four supports of the bridge, namely, the support on the extreme left in Fig. 12 was fixed in all three directions, and the other three supports were on rollers, i.e., their vertical displacements were zero, but they were free to move in a horizontal plane.

With 27 bays in the 3-span double-truss bridge, there were 2×28 nodes in its upper chords. In Fig. 14, we applied a concentrated load of 10,000 lbf at each of the 52 internal upper chord nodes and 5,000 lbf at each of the 4 end upper chord nodes. Total load on the model bridge was $52 \times 10,000 + 4 \times 5,000 = 540,000$ lbf. A rough estimate of the total length of the 466 chords yields a value of about 25,000 in., and a volume of $2.25 \times 25,000 = 56,250$ cu. in. With the density of steel equal to 0.28 lb/cu in, the weight of the model bridge was about 15,750 lbf, or about 3% of the total load in our analysis. We were, therefore, justified to neglect the distributed load effect of the weight of the bridge by assuming it is massless.

The first result of the FEM simulation of the forces in all 466 chords of the **Model-1** bridge is given in Fig. 15. As expected, the lower chords near one of the middle supports were highly stressed. As shown in Fig. 16, we found **Chord 608** to have the maximum compressive force of -88.9 kpf, which exceeds 86.5 kpf, the Euler buckling load. Emulating what we did with the square grillage in the last section, we removed **Chord 608** and performed the FEM analysis again for a 465-chord bridge named **Model-1a**. In Fig. 17, the simulation result showed that **Chord 709** had the maximum compressive force of -121.8 kpf, which again failed the buckling test. So we removed **Chord 709** and performed the FEM analysis again for a 464-chord bridge named **Model-1b**. In Fig. 18, the simulation result showed that a shorter **Chord 845** had the maximum tensile force of +132.2 kpf, which exceeded the tensile yield strength, $Y * A = 36.0 \times 2.25 = 81.0$ kpf. So **Chord 845** broke and the bridge collapsed.

Conclusion: This single simulation ($N = 1, M = 466$) predicted that $n_1 = 1, m = 1$, and $RBI = 0$. **Model-1** is not robust.

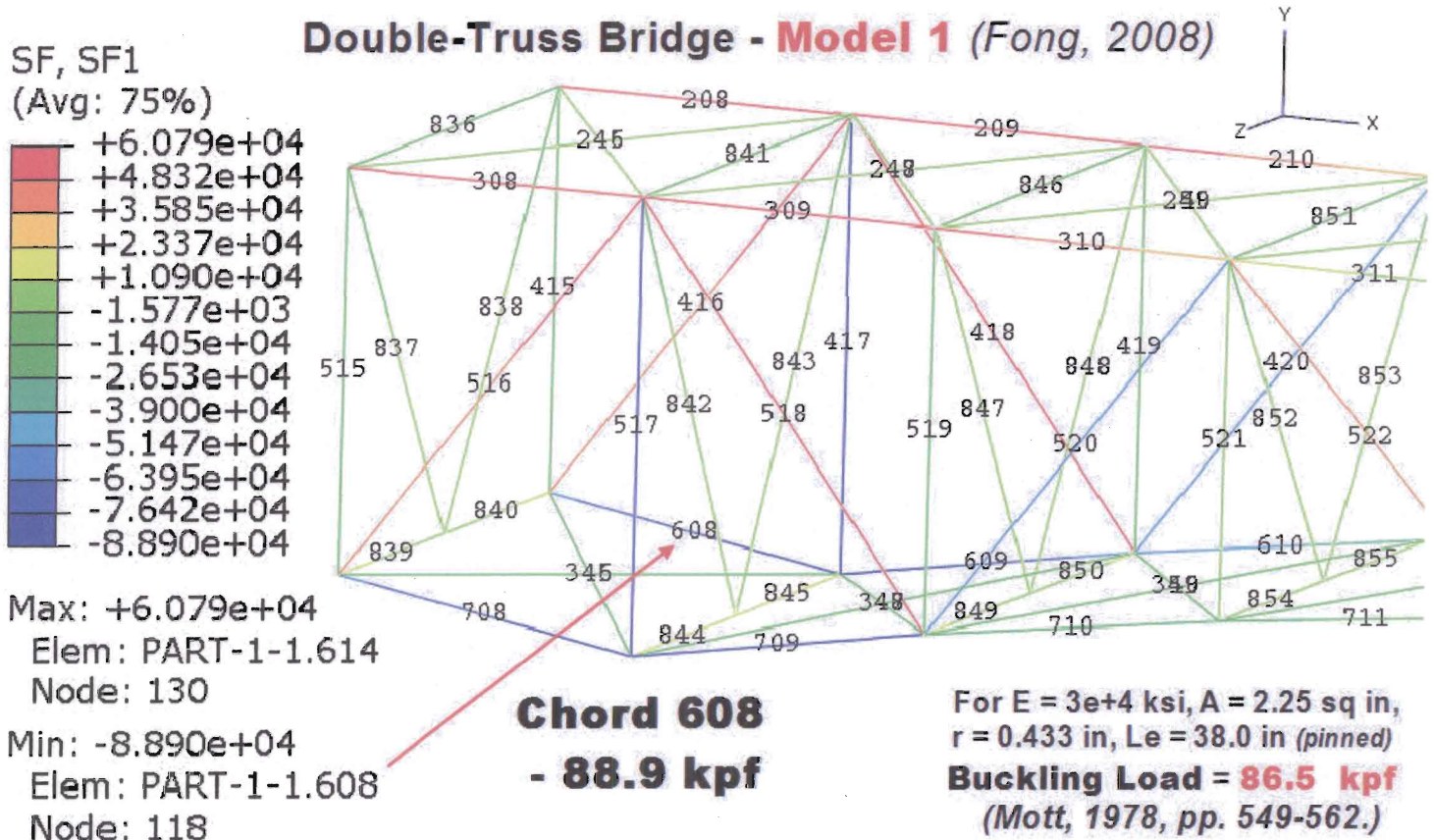


Fig. 16. Key result of a FEM simulation (ABAQUS-SE, v. 6.6.2) of the forces in a portion of the 466-chord **Model-1** bridge, where the Chord 608 was identified as having the maximum compressive force of -88.9 kpf, which exceeded the Euler buckling load.

3. A 466-CHORD DOUBLE-TRUSS BRIDGE (Continued)

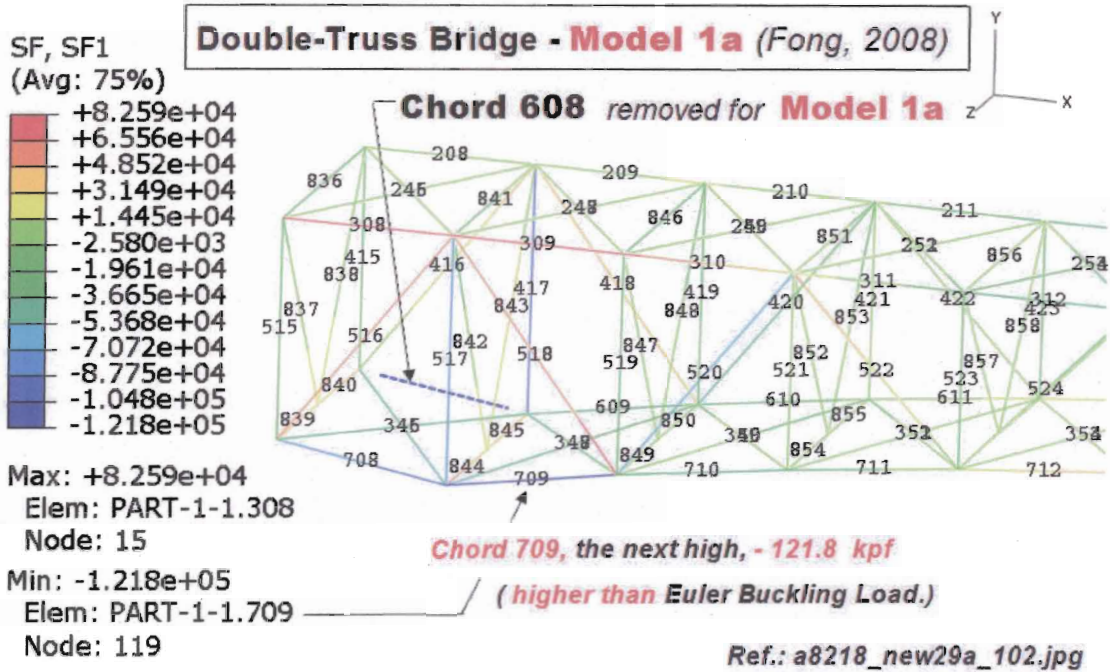


Fig. 17. Key result of a FEM simulation (ABAQUS-SE, v. 6.6.2) of the forces in a portion of the 465-chord **Model-1a** bridge, where the Chord 709 was identified as having the maximum compressive force of -121.8 kpf, which again exceeded the Euler buckling load.

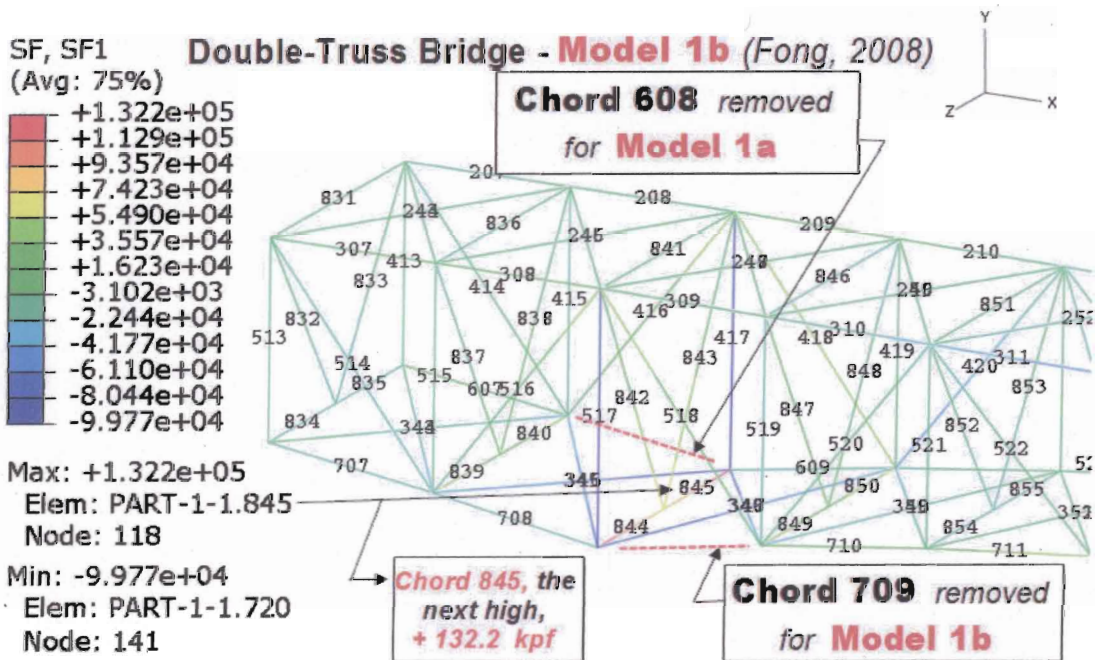


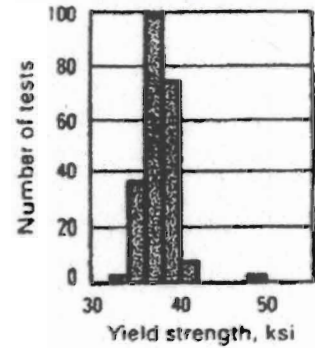
Fig. 18. Key result of a FEM simulation (ABAQUS-SE, v. 6.6.2) of the forces in a portion of the 464-chord **Model-1b** bridge, where the Chord 845 was identified as having the maximum tensile force of +132.2 kpf, which exceeded the tensile yield strength of +81.0 kpf.

3. A 466-CHORD DOUBLE-TRUSS BRIDGE (Continued)

Table 1. Distribution of Room Temperature Yield Strength of A285 Steel, Grade C plates, 6 to 50 mm (1/4 to 2 in.) thick, as purchased from 6 mills with 224 heats by one fabricator during a period of 8 years (Fletcher [12])

Room Temperature Yield Strength Y_o (ksi)	No. of Heats
33	3
35	37
37	99
39	74
41	8
43	0
45	0
47	0
49	3

Fig. 19. A histogram plot of the room temperature yield strength data given by Table 1 on the left for A285 Steel Grade C plates 6 to 50 mm (1/4 to 2 in.)



Heat-to-Heat Variation, ASTM A285 Grade C Steel

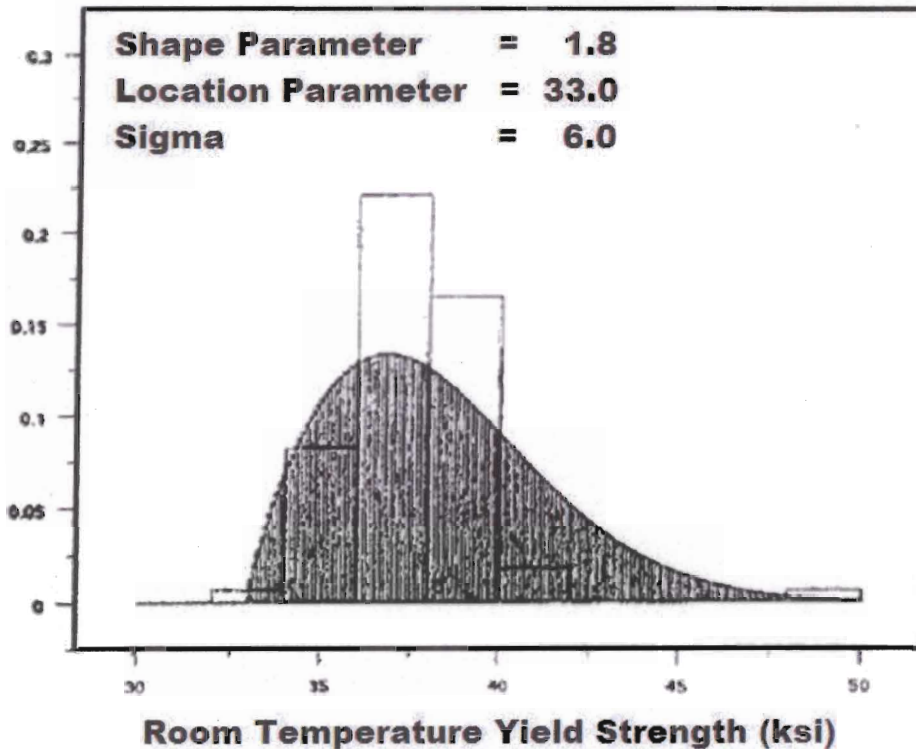


Fig. 20. A Weibull fit of the 224 data points given in Table 1 for the heat-to-heat variation of the room temperature yield strength of 6 to 50 mm (1/4 to 2 in.) thick ASTM A285 Grade C steel plates.

3. A 466-CHORD DOUBLE-TRUSS BRIDGE (Continued)

Fig. 21. Young's Modulus of AISI 4340 and comparables of ASTM A36 Steels at temperatures 20 C to 685 C (Timken [13], ASM [14]). Note that the mean Young's Modulus of 4 samples at 20 C = 30,200,000 psi (see Fong, et al [15])

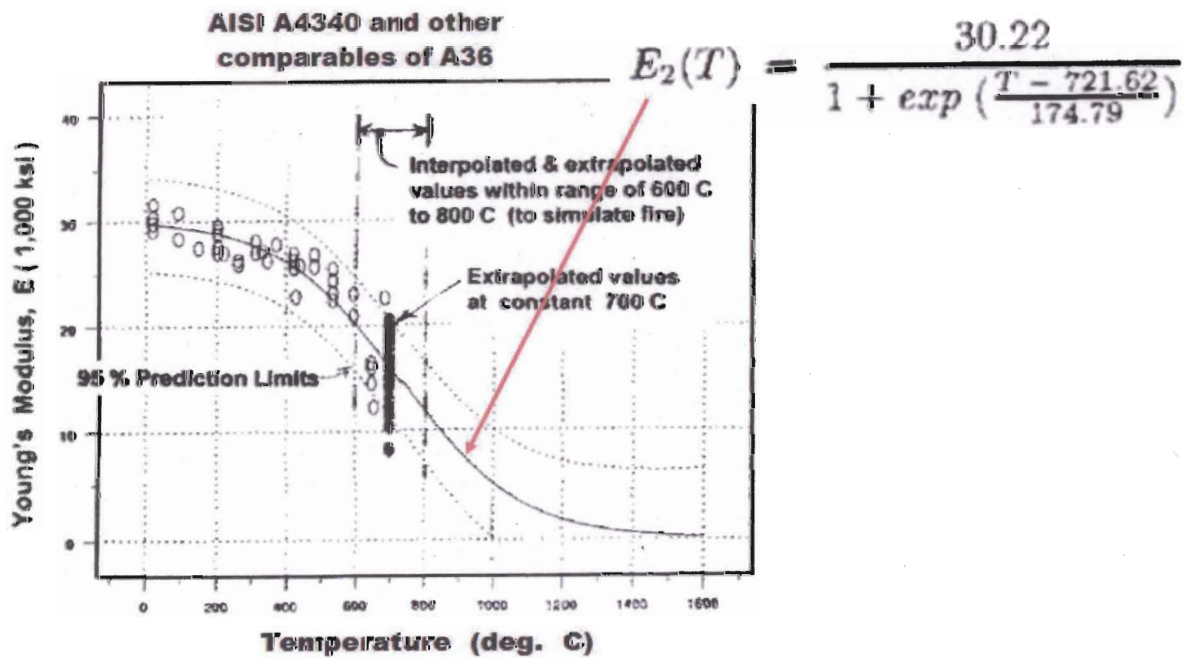
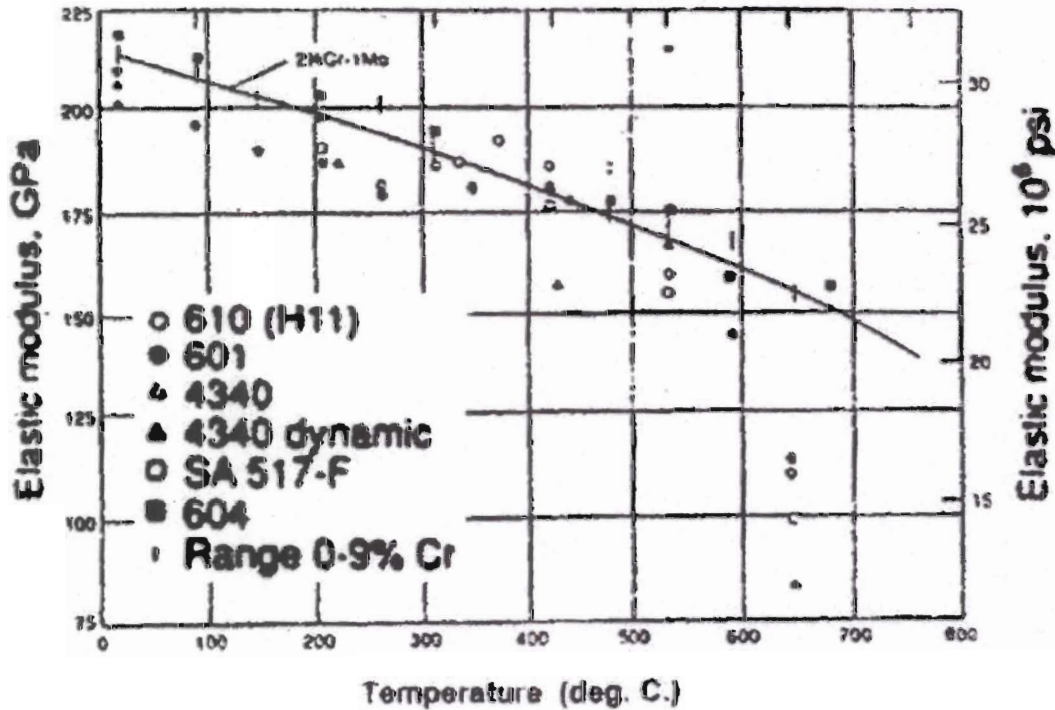


Fig. 22. A Logistic Function Model by Fong et al [15] for Young's Modulus of AISI 4340 Steel and several others comparable to ASTM A36, at temperatures from room to about 1600 C. The raw data appeared in Timken [13] and were reproduced on page 628 of ASM [14].

3. A 466-CHORD DOUBLE-TRUSS BRIDGE (Continued)

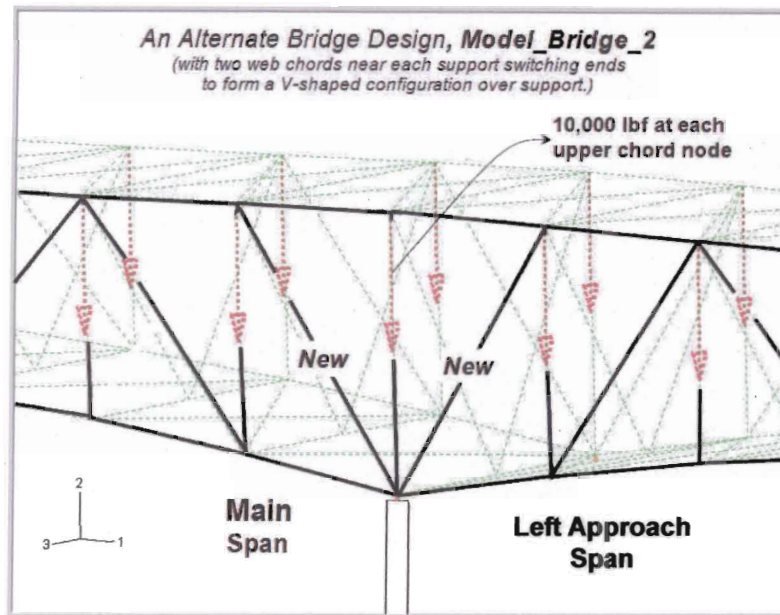


Fig. 23. A perspective view of a portion of the model bridge, **Model-2**, between its Main and Right Approach spans, with a concentrated load of 10,000 lbf applied at each of its upper chord nodes except four at the two ends (not shown), at which only 5,000 lbf is applied.

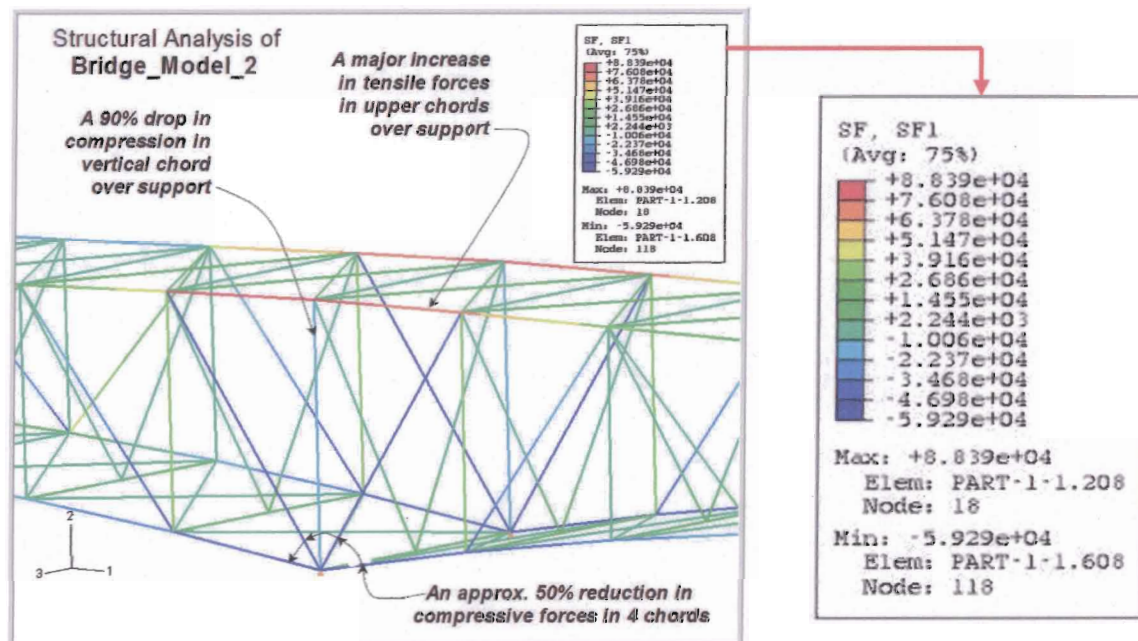


Fig. 24. A perspective view of a portion of the model bridge, **Model-2**, between its Main and Right Approach spans, with results of an analysis by finite element method (ABAQUS, 6.6-2) given in colors, red, orange, yellow being tensile forces, and green, blue, compressive.

3. A 466-CHORD DOUBLE-TRUSS BRIDGE (Continued)

To carry out a statistical FEM simulation experiment for the model bridge, we need to vary two material property parameters, namely, the yield strength, Y , and the Young's modulus, E , because the failure criteria are: (1) Maximum tensile force not to exceed $+Y*A$. (2) Maximum compressive force not to exceed the smaller of the two, $-Y*A$ or P_{Cr} , with P_{Cr} depending on E , A , L_e , and r , according to eq. (2).

In Table 1, we show the heat-to-heat variation of Y at room temperature in 224 heats of ASTM A285 Grade C steel plates, 6 to 50 mm (1/4 to 2 in.) thick, according to Fletcher [12]. A histogram of that data is given in Fig. 19. A Weibull fit of those 224 data points is given in Fig. 20.

In Fig. 21, we reproduce a plot of 37 data points due to Timken [13] and ASM [14] to show the variation of E at temperatures 20 C to 685 C. In Fig. 22, we show a plot of a Logistic Function model by Fong, et al [15] for the Young's modulus of AISI 4340 steel and several others comparable to ASTM A36, at temperatures from room all the way to the melting point of steel. Using the Weibull fit of Y , the Logistic fit of E , and a random number generator in DATAPLOT, we perform N simulations of the model bridge collapse by repeating the single one reported earlier. Results of this statistical FEM failure analysis of a model bridge will appear in a future paper [16].

Having proved the feasibility of the "robustness index" concept for a fixed geometry of a complex structure such as a double-truss bridge, we wish to investigate whether the same concept is applicable to an assessment task when a structure with a variety of geometrical designs is being critically evaluated.

In Fig. 23, we propose an alternate design, named Model-2, where the two cross chords near each of the middle supports (see Fig. 13 for Model-1) assume different positions such that they point directly toward the support instead of away in Model-1. In Fig. 24, we show that, compared to the force distribution in Model-1, there is an approximately 50% reduction in compressive forces in two lower chords and two diagonal chords near support, a 90% drop in compressive forces in a vertical chord over support, but a major increase in tensile forces in upper chords over support. This causes Chord 208 to have a tensile force of +88.39 kpf, which exceeds the tensile yield strength of +81.0 kpf. So we remove Chord 208, and perform a simulation for Model-2a as shown in Fig. 25. The next one to go is Chord 308. In Fig. 26, we remove Chord 308 and perform another FEM simulation for Model-2b. The legend shows that this time, it is Chord 309. In Fig. 27, we found another weak chord over a second middle support in the name of Chord 220 (max. force, 92.05 kpf), which then broke simultaneously with Chord 309 to cause bridge collapse.

Conclusion: From a single simulation, Model-2 is not robust.

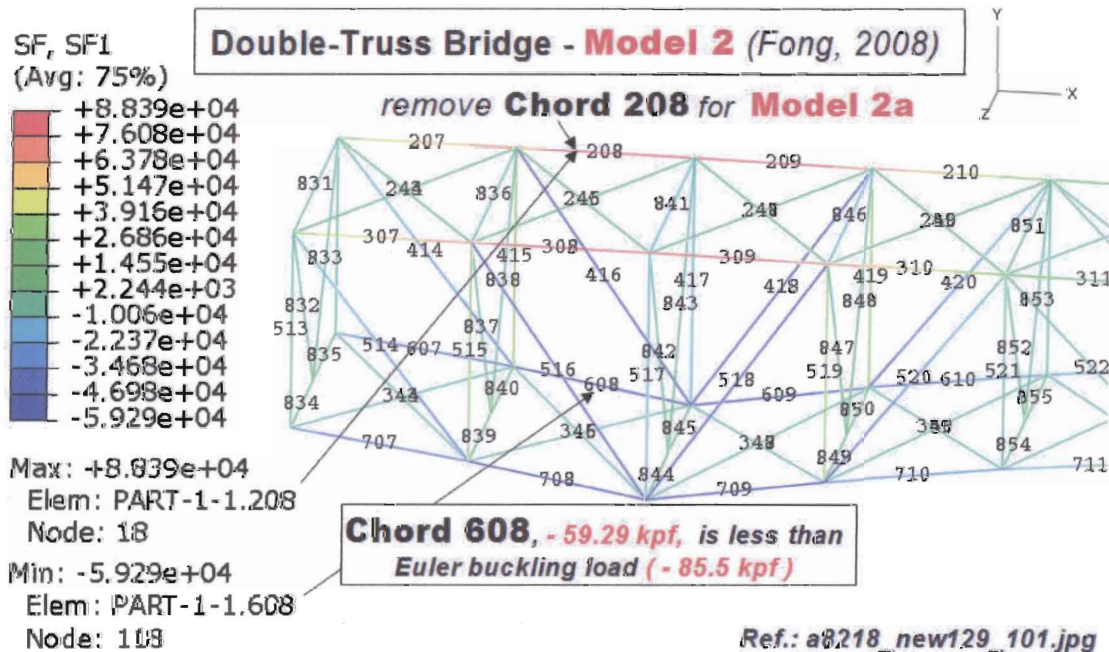


Fig. 25. Key result of a FEM simulation (ABAQUS-SE, v. 6.6.2) of the forces in a portion of the 466-chord Model-2 bridge, where the Chord 208 was identified as having the maximum tensile force of +88.39 kpf, which exceeded the tensile yield of +81.0 kpf.

3. A 466-CHORD DOUBLE-TRUSS BRIDGE (Continued)

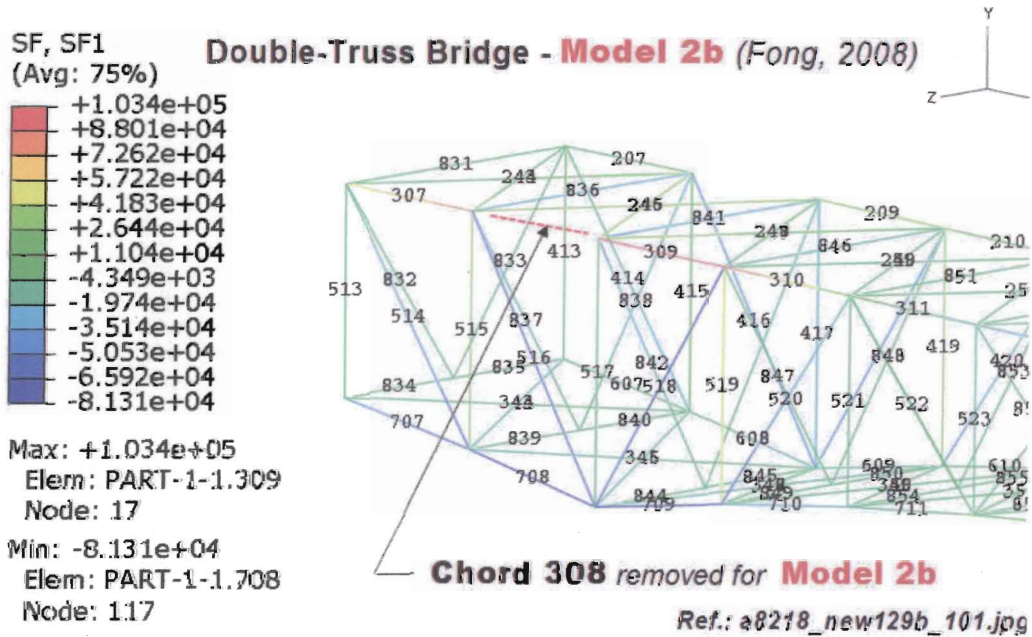


Fig. 26. Key result of a FEM simulation of the forces in a portion of the 464-chord Model-2b bridge, where the Chord 309 was identified from the legend as having the maximum tensile force of + 103.4 kpf, exceeding the tensile yield of +81.0 kpf.

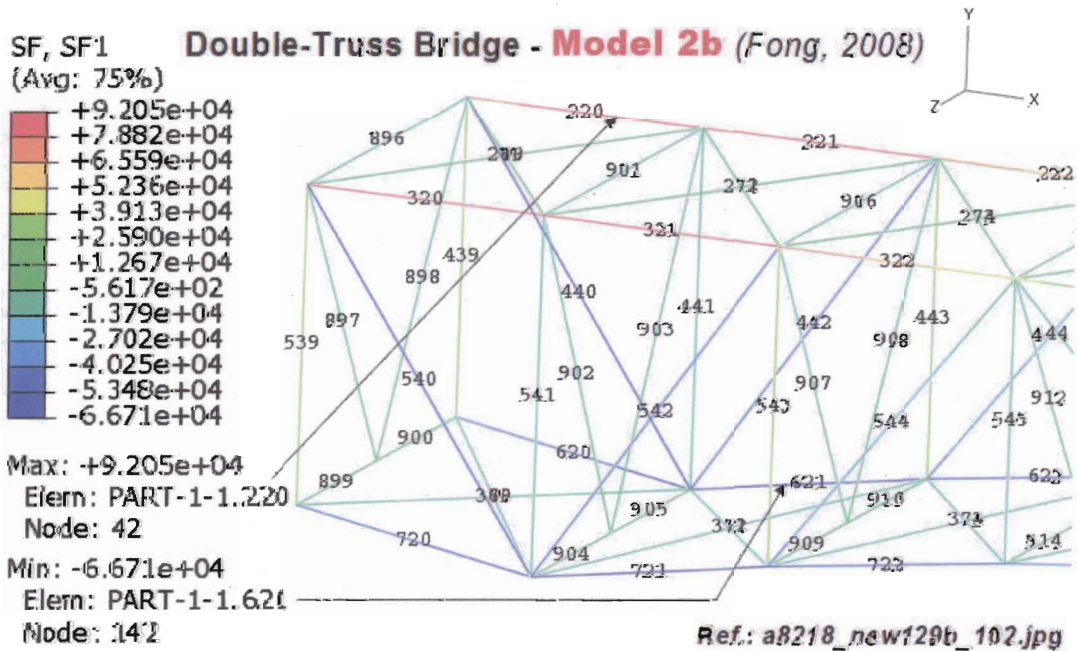


Fig. 27. Key result of a FEM simulation of the forces in a portion of the 464-chord Model-2b bridge, where the Chord 220 was identified from the legend as having the maximum tensile force of + 92.05 kpf, exceeding the tensile yield of +81.0 kpf.

3. A 466-CHORD DOUBLE-TRUSS BRIDGE (Continued)

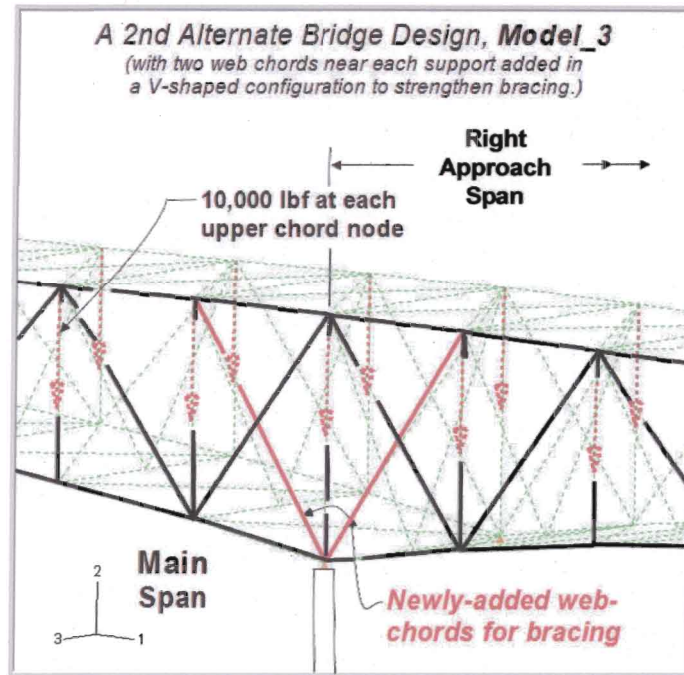


Fig. 28. A perspective view of a portion of the model bridge, **Model-3**, between its Main and Right Approach spans, with a concentrated load of 10,000 lbf applied at each of its upper chord nodes except four at the two ends (not shown), at which only 5,000 lbf is applied.

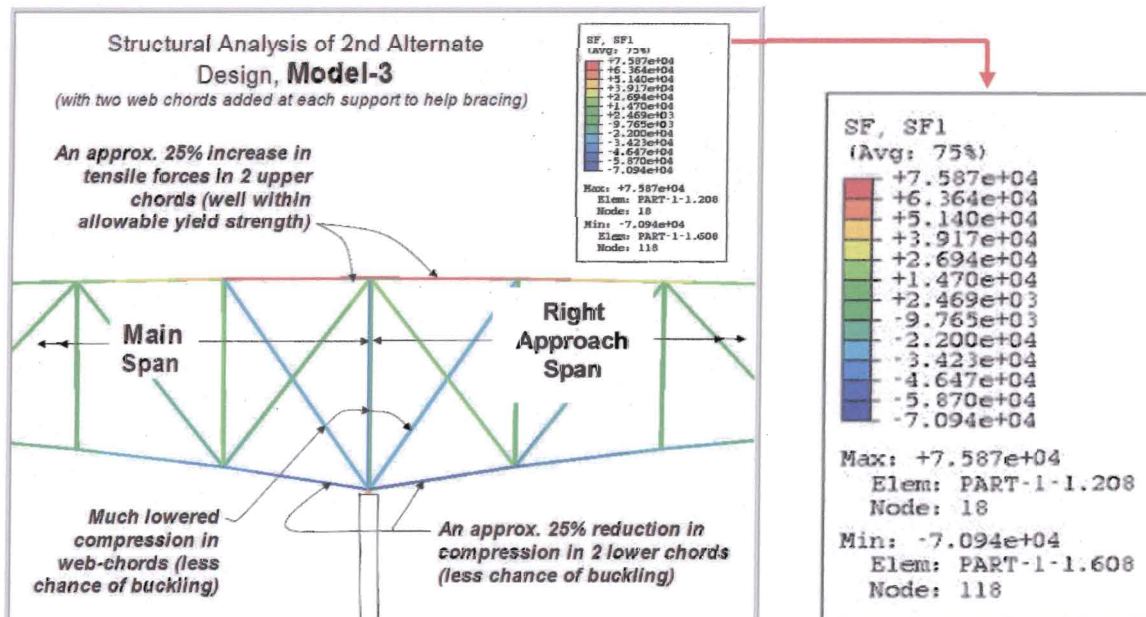


Fig. 29. A perspective view of a portion of the model bridge, **Model-3**, between its Main and Right Approach spans, with results of an analysis by finite element method (ABAQUS, 6.6-2) given in colors, red, orange, yellow being tensile forces, and green, blue, compressive.

3. A 466-CHORD DOUBLE-TRUSS BRIDGE (Continued)

Having performed two single simulations for **Model-1** and **Model-2**, both with disastrous results on their robustness, it is interesting to ask whether another alternate design, named **Model-3**, with cross web chords near support, will fare better.

In **Fig. 28**, we show the geometry of the new design with eight extra chords (474-chord **Model-3**). We have now departed from the constraint of a fixed total mass of the structure for a fair evaluation of alternate designs, but it is instructive to do so because the increase is less than 2% and the result is dramatic.

In **Fig. 29**, we observe that the force distribution in **Model-3** is significantly more balanced. When compared with that of **Model-1**, we see a 25% reduction in compressive forces in two lower chords (less chance of buckling), considerable reduction in compressive forces in two web chords, and a 25% increase in tensile forces in 2 upper chords well within the allowable yield strength.

In **Fig. 30**, we identify **Chord 208** with the maximum tensile force of +75.87 kpf, which is less than the mean tensile yield of +81.0 kpf. We also identify **Chord 608** with the maximum

compressive force of -70.94 kpf, which is less than the Euler buckling load of 86.5 kpf. So the structure is stable as is. For a single simulation, $N = 1$, $n_1 = 0$, $M = 474$, $m = \text{indeterminate}$, and RBI is close to 100.

Let us conduct a 2-simulation experiment with both the tensile yield strength, Y , and the Young's modulus, E , assumed as random variables with distributions given by **Figs. 20** and **22**, respectively. For the first simulation, let us assume that Y is less than the mean strength (+81.0), and **Chord 208** breaks to force **Model-3** to a 473-chord **Model-3a** (see **Fig. 31**). The results of the simulation on **Model-3a** are given in **Fig. 32**, where **Chord 308** is found to have the maximum tensile force of +82.0, about 1% over the mean tensile yield (+81.0). Whether **Chord 308** survives or not, we now have at least one case where the structure passes the "initial resilience" test by not failing at the loss of the first chord. After we conduct the second simulation with very similar results, we are now able to compute m , the mean of the first failing chords of both simulations, and arrive at the following interesting result:

Conclusion: For $N = 2$, $n_1 = 0$, $M = 474$, and $m = 2$, we have $RBI = 99.6$. **Model-3** is robust, pending verification by additional N -simulation experiments with $N > \text{or} = 10$.

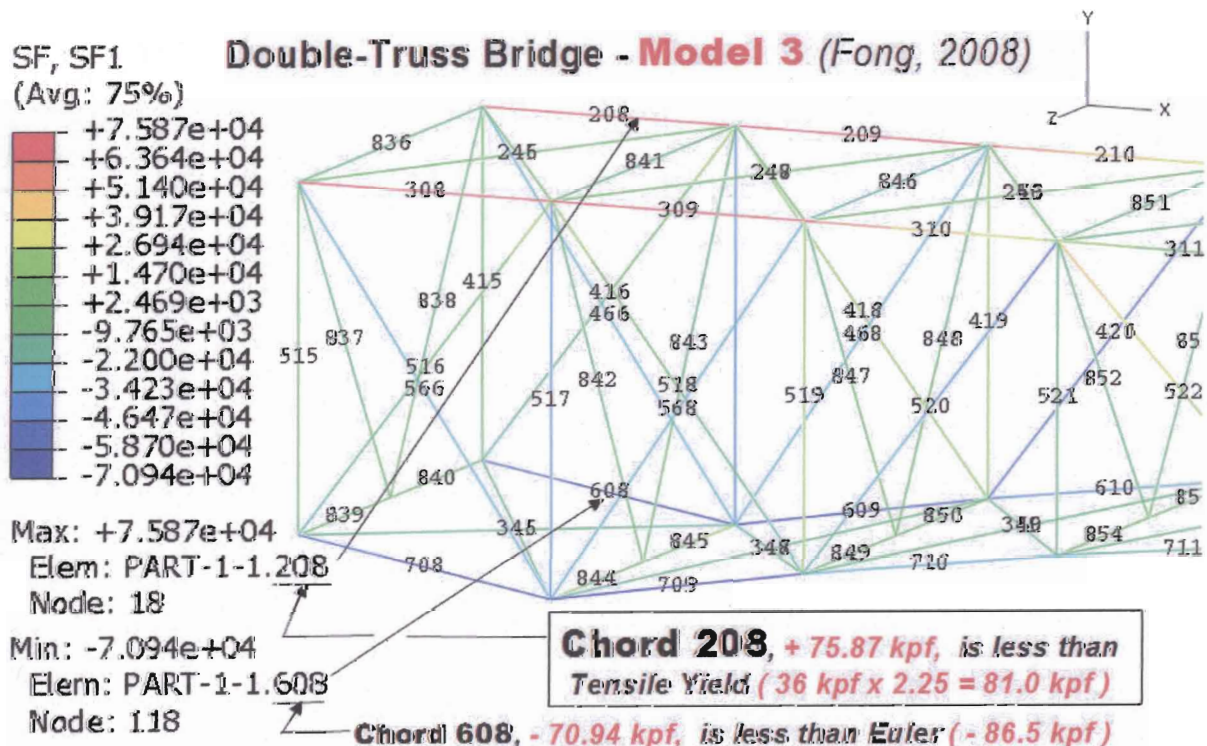


Fig. 30. Key result of a FEM simulation (ABAQUS-SE, v. 6.6.2) of the forces in a portion of the 474-chord **Model-3** bridge, where the **Chord 208** was identified as having the maximum tensile force of +75.87 kpf, which is less than the tensile yield of +81.0 kpf.

3. A 466-CHORD DOUBLE-TRUSS BRIDGE (Continued)

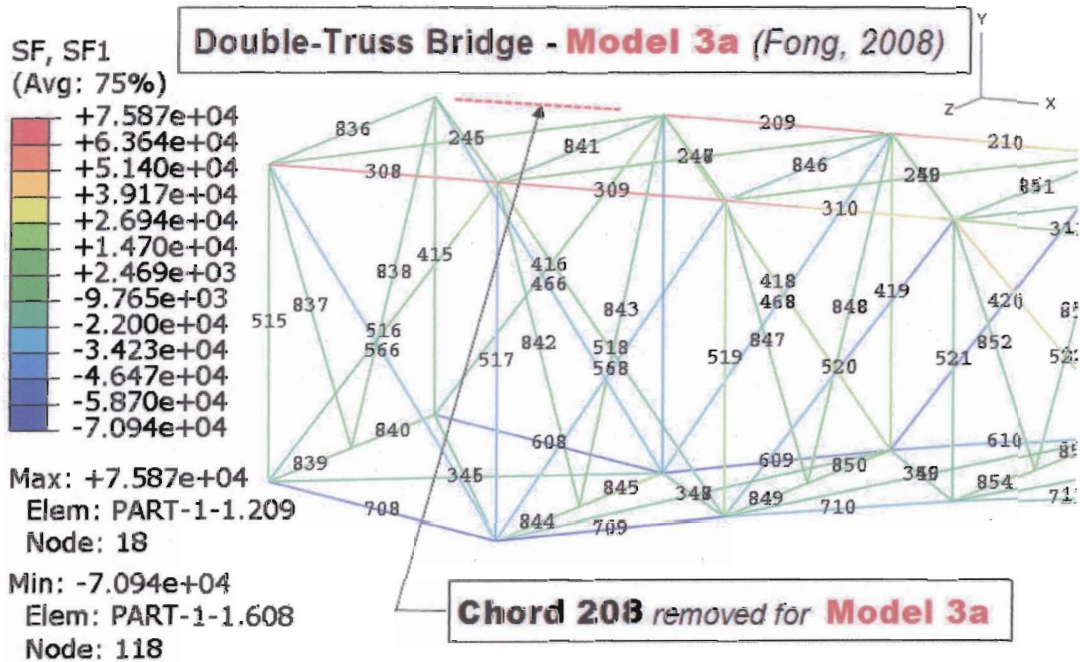


Fig. 31. Key result of a FEM simulation (ABAQUS-SE, v. 6.6.2) of the forces in a portion of the 473-chord Model-3a bridge, where the Chord 208 was removed in a statistical experiment with yield strength as one of two random variables in the formulation.

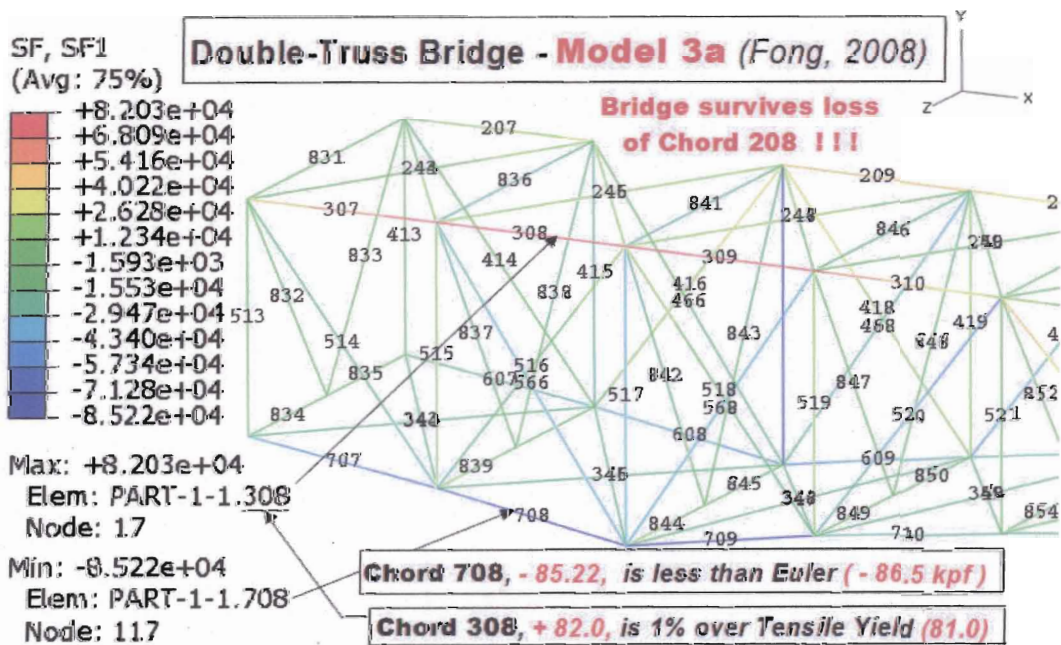


Fig. 32. Key result of a FEM simulation (ABAQUS-SE, v. 6.6.2) of the forces in a portion of the 473-chord Model-3a bridge, where the Chord 308 was identified to have a maximum tensile force of +82.0 kpf, one percent over the mean tensile yield of +81.0.

4. SIGNIFICANCE AND LIMITATIONS OF "RBI"

Engineers have known for a long time that all structures age, and most high-consequence structures are protected from catastrophic failure by a carefully designed periodic or continuous inspection program using NDE.

Yet, catastrophic failures of structures still occur, and the question to ask is whether there exists an inexpensive series of "screening" tests for assessing not only the "health" of an aging structure, much like a physical examination of a grown-up person, but also its design features to see how robust it is in handling progressive weakening and sudden on-set of failure.

Since 1970s, the science and technology of NDE have provided the former, but NDE is not inexpensive, and, much like human beings, many operators of high-consequence structures are reluctant to invest adequately on NDE to protect them from catastrophic events. This is where *RBI* comes in handy.

As shown in eq. (1), we define in this paper the "Robustness Index," or, *RBI*, as the product of two factors, one being a measure of the initial resilience, and the other, the overall resilience of a structure after it sustains an initial loss of a part. *RBI* is a statistical concept, not only because it is estimated from the results of a large number of computer simulations based on material property, loading, and geometric parameters with statistical distributions, but also because of an abundant accumulation of scientific evidence that structural failures do not obey a deterministic set of physical laws.

Consequently, as a measure of structural "robustness", *RBI* is also a physical concept that describes a useful property of a new or aging structure. A low index strongly suggests that either an accelerated NDE program or a design change is needed, or both. A high score is likely to provide an owner a reason to apply for a lower premium from an insurance company because of the perceived reduced risk of failure. The development of *RBI* as a new tool to complement NDE is therefore significant because of its simplicity, ease of use, and relatively low cost, as demonstrated in this paper when we used a student edition of a commercially available FEM software package and a public-domain statistical data analysis package.

The concept of *RBI* is not without its limitations. First of all, the user needs to be able to characterize the critical physical parameters of a problem, not as mean values, but as statistical distributions. Secondly, the user needs to "dissect" a structure into distinct parts and to postulate a set of plausible failure scenarios that begin with the loss of one part, followed by a load redistribution and the loss of a second part, another load redistribution and the loss of a third part, and so on. Finally, the user needs to have access to the results of credible and comparable physical experiments for validating the computational model that gives rise to the large number of simulations required to estimate *RBI*.

5. CONCLUSION

A statistical concept of the "robustness" of a structure or component is defined in terms of the results of a large number of simulations of the progressive weakening of a structure under a constant rate of loadings to failure. As a product of two measures of the "resilience" of a structure, one for initial and the other, overall, a robustness index, or, *RBI*, is defined and successfully applied to two examples, one being a "toy" problem as a proof of concept, and the other, a 1/12-scaled double-Pratt-truss bridge motivated by a figure in a bridge design textbook (Tall [5]). In the second example, the index is used to suggest that the addition of eight additional web chords in the two truss bays immediately over each of the main span supports (see Fig. 28, Model-3) may add substantially to the robustness of the bridge and prevent a catastrophic failure.

6. ACKNOWLEDGMENTS

We wish to thank Howard Baum, Ronald F. Boisvert, Richard Fields, Kuldeep Prasad, Ronald Rehm, and Emil Simiu, all of NIST, H. Norm Abramson of Southwest Research Institute, San Antonio, TX, Hal F. Brinson of University of Houston, Houston, TX, Marvin J. Cohn and Geoffrey Egan of Aptech Engineering Services, Sunnyvale, CA, Owen F. Hedden of Codes and Standards Consulting, Fort Worth, TX, Mel F. Kanninen of San Antonio, TX, Poh-Sang Lam of Savannah River National Laboratory, Aiken, SC, Bradley E. Layton of Drexel University, Philadelphia, PA, and Pedro Marcal of MPave Corp., Julian, CA, for their valuable discussions/comments during the course of this investigation.

The work reported here has been supported, in part, by NIST through two intramural grants over a span of three years, namely, (a) a 2003 contract award to the first author (Fong), P. O. No. NA.1341-03-W-0536, entitled "Modeling and Analysis of Structural Integrity of a Complex Structure under Mechanical and Thermal Loading," and (b) a 2004-05 competence award to the first two authors (Fong & Filliben) on "Complex System Failure Analysis: A Computational Science Approach," for which each of the individual awardees is grateful.

7. REFERENCES

- [1] Rossmannith, H. P., 1983, "FPE - Failure Prevention Engineering: Fracture Mechanics Between Designer and Failure Analysis," in Proceedings of the First International Conference on Structural Failure, Product Liability, and Technical Insurance, Vienna, Austria, 26-29 Sep., 1983, edited by H. P. Rossmannith, pp. 11-21. Elsevier (1983).
- [2] PiesoId, D. D. A., 1991, Civil Engineering Practice: Eng. Success by Analysis of Failure. McGraw-Hill (1991).
- [3] Kanninen, M. F., and Popelar, C. H., 1985, Advanced Fracture Mechanics. Oxford University Press (1985).
- [4] Bush, S. H., and Hedden, O. F., 2007, "Flaw Detection, Location, and Sizing," Digest of an ASME Symposium on "Engineering Safety, Applied Mechanics, and Nondestructive Evaluation (NDE)," San Antonio, TX,

- July 25-26, 2007, J. T. Fong and O. F. Hedden, eds., pp. 153-156. Published by Stanford Mechanics Alumni Club, 104 King Farm Blvd, C308, Rockville MD 20850 (2007).
- [5] Tall, L., ed., 1974, Structural Steel Design, 2nd ed., pp. 98-99, Fig. 4.3(b). New York: Ronald Press (1974).
- [6] Filliben, J. J., and Heckert, N. A., 2002, DATAPLOT: A Statistical Design Analysis Software System, a public domain software released by National Institute of Standards & Tech., Gaithersburg MD 20899, <http://www.itl.nist.gov/div898/software/dataplot.html>
- [7] Anon., 2006, ABAQUS User's Manual, Version 6.6-2 (Student Version). Providence, RI: ABAQUS, Inc. (2006).
- [8] Hastings, N. A., and Peacock, J. B., 1975, Statistical Distributions, pp. 124-129 London: Butterworth (1975).
- [9] Evans, M., Hastings, N. A. J., and Peacock, J. B., 2000, Statistical Distributions, 3rd ed., pp. 192-203. Wiley (2000).
- [10] Filliben, J. J., 1975, "The Probability Plot Correlation Coefficient Test for Normality," Technometrics, Vol. 17, No. 1, pp. 111-117 (1975).
- [11] Mott, R. L., 2002, Applied Strength of Materials, 4th ed. (1st ed., 1978, by Pearson Education Inc, Upper Saddle River, NJ 07458). Upper Saddle River, NJ: Prentice-Hall (2002)
- [12] Fletcher, F. B., 1990, "Carbon and Low-Alloy Steel Plate," in Metals Handbook, 10th ed., Vol. 1, pp. 226-239. ASM International, Materials Park, OH 44073 (1990).
- [13] Timken Roller Bearing Company, 1957, Digest of Steels for High Temperature Service, 6th edition (1957).
- [14] ASM International, 1990, Properties and Selection: Irons, Steels, and High Performance Alloys, Metals Handbook, 10th ed., Vol. 1, p. 628. ASM International, Materials Park, OH 44073 (1990).
- [15] Fong, J. T., Filliben, J. J., Fields, R. J., and Bernstein, B., 2002, "A Stochastic Model of the Collapse of Two Simple Steel Grillages in a Fire: Note 1. Material Property Variabilities of Two Steels," Draft Manuscript dated Aug. 25, 2002, an internal working document of the Mathematical and Computational Sciences Division, National Institute of Standards and Technology, Gaithersburg, MD 20899-8910. Available upon request to fong@nist.gov (2002).

APPENDIX A

A SAMPLE DATAPLOT INPUT FILE FOR SIMULATING COLLAPSE OF A 40-COLUMN SQUARE GRILLAGE

```

-----
. Feb. 14, 2008          Filename: fong99.dp
.
. Subject: A DATAPLOT Script File to Compute Collapse
.   Time of a 40-column grillage using both mean-based
.   and stochastic (Weibull, 100 samples) models
.
. By: Jeffrey Fong, James Filliben, and Alan Heckert, NIST
-----
.
let numcol = 40
let loadrate = 1
let string dist = Weibull
let gamma = 1.05
let ppa0 = 2.7883
let ppa1 = 2.5251
let mean = 5.0
let timemba = mean*numcol/loadrate
.
feedback off
.
let numsamp = 100
.
loop for k = 1 1 numsamp
.
  let n = numcol
  let pp = weibull random numbers for i = 1 1 n
  let pp = ppa0+ppa1*pp
  let pp = sort pp
  let index = 1 1 n
  let currcol = n-index+1
  let t = pp*currcol/loadrate
  let maxt = maximum t
  let maxt1 = round(maxt, 1)
  let index2 = index
.
retain index2 subset t maxt
.
  let collcol = index2(1)
  let maxtv(k) = maxt
  let collcolv(k) = collcol
.
if k <= 16
.
  ylim 2.5 5; xlim 70 130
  char x all; char hw 2 1 all; char automatic index; lines
.
  y1label Collapse Load per Column (Ordered); y1label size 3
  x1label Collapse Time (Min.); x1label size 3

```

```

Legend 1 Stochastic Failure of a ^numcol-column Grillage
(Fong-Filliben-Heckert, 2008)
Legend 1 coor 50 94
Legend case asis
Legend 1 just center
Legend 1 size 3.2
.
x3label
.
plot pp t index
.
hw 2.5 1.3
move 16 87; just left; text Total No. of Columns = ^numcol
move 57 87; just left; text Column Mean Strength = ^mean
move 57 83; just left; text Loading Rate = 1.0 per minute
move 57 25.5; just left; text MEAN-BASED Model Result:
move 57 21.5; just left; text Collapse Time = 200.0 Min.
move 16 40; just left; text STOCHASTIC Model Results:
move 16 36; just left
  text Total No. of Simulations = ^numsamp
move 16 32.5; just left; text Random Sample No. ^k
move 16 29; just left; text Collapse Time = ^maxt1 Min.
move 16 25.5; just left
  text Collapse Column ID = ^collcol
move 16 21.5; just left; text Plot Character = Column ID.
.
end if
.
end loop
.
let meantime = mean maxtv
let sdtime = sd maxtv
let medtime = median maxtv
let mintime = minimum maxtv
let mint = round(mintime, 1)
let pctred = mint*100/timemba
let pctreduc = round(pctred, 1)
.
xmaximum timemba
.
char hw 4 2 all; ylimits
x1label Histogram of Collapse Time (Min.); x1label size 3
y1label Counts; y1label size 3
.
histogram maxtv
.
lines dotted; drawdsds timemba 20 timemba 30
char hw 4 2 all
.

```

APPENDIX A (Continued)

```
move 85 13; just left; text Mean-based
move 85 10; just left; text Analysis
lines dotted; draw 84.5 13 80 23; char hw 4 2 all
move 52 77; just left; text STOCHASTIC Model Results:
move 55 73; just left
    text Time to Collapse (^numsamp samples)
move 58 69; just left; text Mean = ^meantime Min.
move 58 65.5; just left; text SD = ^sdtime Min.
move 58 62; just left; text Median = ^medtime Min.
move 55 58; just left; text Minimum Collapse Load
move 64 54.5; just left; text = ^mint
move 55 51; just left; text Load Capacity Reduction
move 64 47.5; just left; text = ^pctreduc %
move 16 87; just left; text Total No. of Columns = ^numcol
move 16 83; just left; text Column Mean Strength = ^mean
move 16 79; just left; text Loading Rate = 1.0 per minute
move 52 87; just left; text MEAN-BASED Model Result:
move 55 83; just left; text Time to Collapse = ^timemba Min.
```

```
let meancc = mean collcolv
let sdcc = sd collcolv
let medcc = median collcolv
```

```
·
xlim 0 numcol; ylim 0 40
x1label Histogram of Number of Failed Columns at Collapse
x1label size 3
y1label Counts; y1label size 3
```

```
·
histogram collcolv
```

```
·
char hw 4 2 all
move 45 87; just left
    text Total No. of Simulations = ^numsamp
move 45 80; just left
    text Let M = Total No. of Columns = ^numcol
move 45 74;; just left; text Let m = Mean = ^meancc
move 55 70.5; just left; text SD = ^sdcc
move 55 67; just left; text Median = ^medcc
move 45 61; just left; text Let n1 = no. of first failed columns
move 55 57.5; just left; text in a ^numsamp-sample
move 45 54; just left; text Let N = sample size
move 45 48; just left; text Let RBI = "Robustness" Index
move 45 44.5; just left
    text where  $RBI = (N-n1)*(M-m)*100 / (N*M)$ 
move 45 41; just left; text with RBI = 100, being the most,
move 45 37.5; just left
    text and RBI = 0, the least "robust."
```

```
line dash
draw 21 58 44 62
erase
```

APPENDIX B

A SAMPLE ABAQUS INPUT FILE FOR ESTIMATING THE CHORD FORCES OF A 466-ELEMENT BRIDGE

```

** -----
** Date: Aug. 20, 2007          Filename: model-1.inp
** By: Jeffrey Fong & Roland deWit, NIST, Gaithersburg MD
**
** Finite Element Code:  ABAQUS 6.6-2 Student Edition
** US Units ( in , lbf, lbf s2/in, s, psi, in lbf, lb s2/in4 )
** for ( Length, Force, Mass, Time, Stress, Energy, Density )
**
** No. of Nodes:      141.    No. of Elements: 466.
** Element: FRAME3D   Material: Linear Elastic (Steel)
** Young's Modulus: 3.0e+7.  Poisson's Ratio: 0.30.
**
** BC_3 = Bound. Cond. Type 3: fixed_roller_roller_roller
** Rod cross section: 1.5-in square, for all 466 rods
** Loading: 10,000 lbf concentrated nodal load at upper chord
**
** WARNING: THIS FILE HAS BEEN ANNOTATED
** FOR EASE OF UNDERSTANDING THE LOGIC OF
** CODE DEVELOPMENT. FOR BREVITY, A FEW
** SECTIONS OF THE CODE HAVE BEEN OMITTED,
** AND THE READER NEEDS TO SUPPLY THE
** MISSING LINES BEFORE SUBMITTING THE FILE
** FOR EXECUTION IN AN ABAQUS ENVIRONMENT.
** -----
**
**Heading
A Double-Truss Bridge_BC_3 (Fong-deWit, 8/20/07)
**
**Preprint, echo=NO, model=NO, history=NO, contact=NO
**
** -----
** Definition of PARTS
** -----
**
**Part, name=PART-1
**
** -----
** NODE Definition: For the double-truss bridge,
** we assume the two trusses to be 60 ft. apart.
** For a 1/12-scale model, they are 60 in. apart.
**
** Front Truss - Left Approach Span
** (8 bays at 38 in. ea)
** Upper chord: 9 nodes ( 1, 17, step 2)
**
** Main Span (12 bays)
** Upper chord: 12 nodes (19, 41, step 2)
**
** Right Approach Span (7 bays)
** Upper chord: 7 nodes (43, 55, step 2)
**
** Front Truss - 3 spans (27 bays)
** Lower chord: 28 nodes (101,155, step 2)
**
** Back Truss - 3 spans (27 bays)
** Upper chord: 28 nodes ( 2, 56, step 2)
**
** Back Truss - 3 spans (27 bays)
** Lower chord: 28 nodes (102,156, step 2)
**
** Laterals - Lower Chord Midpoint In-Between
** 28 nodes (161,188, step 1)
**
** -----
** Total for 2 trusses and in-between: 140 nodes plus
** ONE MORE NODE for defining a 3-D coordinate system.
** -----
**Node
1, -532., 0., 0.
3, -494., 0., 0.
5, -456., 0., 0.
7, -418., 0., 0.
9, -380., 0., 0.
11, -342., 0., 0.
13, -304., 0., 0.
15, -266., 0., 0.
17, -228., 0., 0.
** -----
** Note: Definition of 131 more nodes is omitted for brevity.
** Note: One extra node to define 3-D coordinate system
** -----
200, 0., 0., -1.
** -----
** Element Definition begins
**
** Note: Total 466 Elements defined as follows:
**
** Front Truss - Upper chord: 27 elements
** Web chord: 55 elements
** Lower chord: 27 elements
**
** Back Truss - Upper chord: 27 elements
** Web chord: 55 elements
** Lower chord: 27 elements
**
** Laterals - 28 Portals at 5 elements each: 140 elements
** 27 Upper cross bracings @ 2 each: 54 elements
** 27 Lower cross bracings @ 2 each: 54 elements
**
** -----
** Total No. of elements: 466
** -----

```

APPENDIX B (Continued)

```

**
*Element, type=FRAME3D
**
** -----
** Note: 8+12+7=27 Upper Chords, Front full truss
** -----
** ----- 8 for Left Approach Span
301,3,1
302,5,3
303,5,7
304,7,9
305,9,11
306,11,13
307,13,15
308,15,17
** -----
** Note: Definiton for 458 more elements omitted for brevity.
** -----
** Note: ELEMENT DEFINITION ENDS (466 steel bars
** of 1.5-IN SQUARE CROSS SECTION WITH AREA
** EQUAL TO 2.25 SQ IN TO BE SPECIFIED LATER)
** -----
** Note: DEFINITION OF 35 ELEMENT SETS begins:
**
** Name of first set:  _K1 ( 2 elements),
**                    _K2 ( 2 elements),
**
** and  _K11 (16 elements),
**      _K12 (16 elements),
**      _K13 (16 elements),
**      _K14 (16 elements),
**      _K15 (16 elements),
**      _K16 (16 elements),
**      _K17 (16 elements),
**      _K18 (16 elements),
**      _K19 (16 elements),
**
**      _K20 (15 elements),
**      _K21 ( 8 elements),
**      _K22 ( 8 elements),
**      _K23 ( 8 elements),
**      _K24 ( 7 elements),
**      _K25 ( 8 elements),
**      _K26 ( 8 elements),
**      _K27 (10 elements),
**
**      _K28 (16 elements),
**      _K29 (16 elements),
**      _K30 (16 elements),
**      _K31 (16 elements),
**      _K32 (16 elements),

```

```

**      _K33 (16 elements),
**      _K34 (16 elements),
**      _K35 (16 elements),
**      _K36 (16 elements),
**      _K37 (16 elements),
**      _K38 (16 elements),
**      _K39 (14 elements),
**
**      _K41 (14 elements),
**      _K42 (14 elements),
**      _K43 (14 elements),
**      _K44 (14 elements),
**
** using 2 commands named "Elset" and "Frame Section",
** where Elset. with Frame Section denotes a special
** boundary condition for each element, namely, pinned,
** which is default for elements with uniaxial response
** -----
**
*Elset, elset= _K1, internal
201,202
**
*Frame Section, elset= _K1, section=RECT
1.5, 1.5
0.,0.,-1.
3.0e+7, 1.154e+7
**
** ----- ELSET ( _K2)
**
*Elset, elset= _K2, internal
301,302
**
** Section: Section-1 Profile: Profile-1
**
*Frame Section, elset= _K2, section=RECT
1.5, 1.5
0.,0.,-1.
3.0e+7, 1.154e+7
**
** ----- ELSET ( _K11)
**
*Elset, elset= _K11, internal
203,204,205,206,207,208,209,210,211,212,213,214,215,216,2
17,218
*Frame Section, elset= _K11, section=RECT
1.5, 1.5
0.,1.,0.
3.0e+7, 1.154e+7
**
** -----
** Note: Definition of elsets _K12 thru _K39 omitted for
brevity
** -----

```

APPENDIX B (Continued)

```
** -----
** Note: CHANGE 2nd line on VECTOR FOR NEXT
**       FOUR ELSETS of Verticals
** -----
**
*Elset, elset=_K41, internal
401,403,405,407,409,411,413,415,417,419,421,423,425,427
*Frame Section, elset=_K41, section=RECT
1.5, 1.5
1.,0.,0.
3.0e+7, 1.154e+7
**
*Elset, elset=_K42, internal
429,431,433,435,437,439,441,443,445,447,449,451,453,455
*Frame Section, elset=_K42, section=RECT
1.5, 1.5
1.,0.,0.
3.0e+7, 1.154e+7
**
*Elset, elset=_K43, internal
501,503,505,507,509,511,513,515,517,519,521,523,525,527
*Frame Section, elset=_K43, section=RECT
1.5, 1.5
1.,0.,0.
3.0e+7, 1.154e+7
**
*Elset, elset=_K44, internal
529,531,533,535,537,539,541,543,545,547,549,551,553,555
*Frame Section, elset=_K44, section=RECT
1.5, 1.5
1.,0.,0.
3.0e+7, 1.154e+7
**
*End Part
**
** -----
**
*Assembly, name=Assembly
**
*Instance, name=PART-1-1, part=PART-1
**
*End Instance
**
** -----
**
** Note: DEFINITION OF 7 NODE SETS begins
**
** Name of first node set:  _M4 (6 NODES, U2=0),
**
** second node set:  _M5 (2 NODES, Fully-Fixed),
**
** third node set:  _M6 ( 4 NODES, half-load),
```

```
**
** and 4 more:  _M7 (13 NODES, full-load),
**             _M8 (13 NODES, full-load),
**             _M9 (13 NODES, full-load),
**             _M10 (13 NODES, full-load),
**
** WHERE _M4 and _M5 are for boundary cond.,
**
** AND _M6 and _M7 to _M10 are for loading cond..
**
*Nset, nset=_M4, internal, instance=PART-1-1
117,118,141,142,155,156
**
*Nset, nset=_M5, internal, instance=PART-1-1
101,102
**
** --- ABOVE FOR B.C.
**
** --- BELOW FOR LOADING CONDITIONS
**
*Nset, nset=_M6, internal, instance=PART-1-1
1,2,55,56
**
*Nset, nset=_M7, internal, instance=PART-1-1
3,4,5,6,7,8,9,10,11,12,13,14,15
**
*Nset, nset=_M8, internal, instance=PART-1-1
16,17,18,19,20,21,22,23,24,25,26,27,28
**
*Nset, nset=_M9, internal, instance=PART-1-1
29,30,31,32,33,34,35,36,37,38,39,40,41
**
*Nset, nset=_M10, internal, instance=PART-1-1
42,43,44,45,46,47,48,49,50,51,52,53,54
**
*End Assembly
**
** -----
** Note: Material Definiton begins
** -----
**
*Material, name=Material-1
**
*Elastic
3.0e+7, 0.3
**
** ----- Make E, Young's Modulus, a random variable
**             to formulate a stochastic model
**
** STEP: Step-1
**
*Step, name=Step-1, perturbation
10000 lbf conc. load at upper chord nodes internal
**
```

APPENDIX B (Continued)

```
*Static
**
*Boundary
_M4, 2
**
*Boundary
_M5, Encastre
**
*Clload
_M6, 2, -5000.
**
*Clload
_M7, 2, -10000.
**
*Clload
_M8, 2, -10000.
**
*Clload
_M9, 2, -10000.
**
*Clload
_M10, 2, -10000.
**
*Output, field, variable=PRESELECT
**
*Node Output
COORD, U, CF, RF, TF
**
*Output, field, variable=PRESELECT
**
*Element Output, directions=YES
SEE, SF
**
*End Step
**
```